NTNU
Norwegian University of
Science and Technology

The impact of high CO2 and low pH on the organic carbon characterization.

Dunia Rios Yunes

Marine Coastal Development
Submission date: May 2018
Supervisor: Nicole Aberle-Malzahn, IBI
Co-supervisor: Murat V. Ardelan, IKJ

Norwegian University of Science and Technology
Department of Biology

Abstract

The atmospheric concentration of carbon dioxide (CO_2) is increasing. Carbon capture and storage (CCS) provides a means to halt emissions. CCS under the seabed has some associated risks, such as seepage of CO_2 from the storage site that in turn can cause localized ocean acidification (OA). The OA affects the marine chemistry and the different species of marine dissolved organic carbon (DOC) as well as the DOC transformation of the marine bacteria. These changes could potentially alter the long-term carbon storage capacity of the ocean. The CO_2Marine project aimed to study the changes in the marine chemistry and bacterial degradation under high-pressure, long-term, low pH conditions. In this thesis, the intention was to study the effect that the low pH conditions would have on the DOC and the bacterial activity and to characterize the different DOC species with liquid chromatography- mass spectrometry (LC-MS). What we found was a decrease in the concentration of DOC and particulate organic carbon (POC) under low pH stress. The DOC compounds characterized were different between treatments and showed an apparent shift from negatively charged to positively charged. There was a higher bacterial degradation activity after low pH stress however; a decreased amount of recalcitrant DOC (RDOC) was produced. 11 potentially RDOC compounds were identified.

Dedication

To my parents, Laila and Octavio, my brother Sebastián, and myself

“In one drop of water are found all the secrets of all the oceans”

Khahlil Gibran

Acknowledgements

I would like to thank professors Murat Van Ardelan and Nicole Aberle Malzahn for giving me the opportunity of collaborating with them, supervising and guiding me. I have learned a lot from them.

Special thanks to Dr. Ana Borrero Santiago for all the support and experience she has shared with me, she has been a great example and is someone to look up to. Dr. Ana always encouraged me to do my best and taught me to see difficulties as opportunities; my master studies would not have been this great without her.

To Dr. Susana Villa Gonzalez and Dr. Tomasz Maciej Ciesielki, they were fundamental for the creation of this thesis; they were always willing to help me and guide me.

To Mathew Kuttivadakkethil Avarachen and all the other people of the environmental chemistry team, SeaLab, and Trondheim´s biological station

To Zachary W. Burnside for supporting me, always making me laugh, and proofreading my thesis.

Table of contents

List of Tables

List of Tables in Appendix

List of Figures

List of Figures in Appendix

List of Abbreviations

Ω	Saturation state
Δ	Delta value
atm	Atmosphere
BCP	Biological carbon pump
BD	Bacterial decomposition
CCS	Carbon capture and storage
CRAM	Carboxyl - rich alicyclic molecules
DIC	Dissolved inorganic carbon
DOC	Dissolved organic carbon
DOC/C	Dissolved organic carbon characterization
HMW	High molecular weight
IAP	Ionic activity product
IQR	Inter quartile range
IR-MS	Isotope ratio - mass spectrometry
K_{sp}	Apparent solubility product
LC-MS	Liquid chromatography - mass spectrometry
LDOC	Labile dissolved organic carbon
LMW	Low molecular weight
MCL	Microbial carbon loop
MCP	Microbial carbon pump
MW	Molecular weight
NMR	Nuclear Magnetic Resonance Spectroscopy
OA	Ocean acidification

OC	Organic carbon
PC	Principal component
PCA	Principal components analysis
$\boldsymbol{pCO_2}$	Partial pressure of carbon dioxide
POC	Particulate organic carbon
RDOC	Refractory dissolved organic carbon
S	Salinity
SLDOC	Semi labile dissolved organic carbon
SPE	Solid phase extraction
SRDOC	Semi refractory dissolved organic carbon
T	Temperature
TA	Total alkalinity
TEP	Transparent exopolymer particles
TiTank	Titanium tank
TOC	Total organic carbon
URDOC	Ultra refractory dissolved organic carbon

1 Introduction

Since the beginning of the industrial revolution, emissions of carbon dioxide (CO_2) in the atmosphere have been increasing steadily (Sabine, 2004; Doney et al., 2009). CO_2 is one of the main greenhouse gases and it is emitted by the combustion of fossil fuels and renewable fuels, deforestation practices, cement production, and transportation, among others (Herzog and Golomb, 2004; Sabine, 2004; Metz et al., 2005). CO_2 has a long atmospheric lifetime, and as such, when it is released into the atmosphere it lingers in it leading to long-term accumulation (Karl, 2003).

The concentration of CO_2 has soared from pre-industrial levels of 278 ppm to current levels of 406 ppm in February 2017 measured by the NOAA Mauna Loa Station (National Oceanic and Atmospheric Administration, 2017).

This increase concentration has resulted changes in the atmosphere, leading to global warming; but it has also affected the oceans, since about 30% of the CO_2 that is absorbed by the oceans and seas, thus altering the marine chemistry and causing a drop in the seawater pH (Brewer, 1997; Sabine, 2004; Fabry et al., 2008; Doney et al., 2009; Feely et al., 2009). One of the major mitigation methods for the raising concentration and accumulation of CO_2 in the atmosphere is the Carbon Capture and Storage (CCS) (Gibbins and Chalmers, 2008). However, there are some risks associated with CCS such as seepage of CO_2 from the storage site (Gibbins and Chalmers, 2008).

2 Theory

2.1 Carbon Capture and Storage (CCS)

There is a current incentive for the use of CCS techniques because they allow us to continue using fossil fuels whilst reducing the CO_2 emissions (Herzog and Golomb, 2004). The advantages of implementing CCS include: the sequestration of CO_2 from the source of emission, long-term storage, a decrease in the atmospheric CO_2 concentration, and enhanced oil and gas recovery (Herzog and Golomb, 2004; Metz et al., 2005; Gibbins and Chalmers, 2008).

CCS involves several steps, such as the collection, concentration, transportation, and long-term storage of CO_2 in the storage sites (Herzog and Golomb, 2004; Metz et al., 2005; Gibbins and Chalmers, 2008; Haszeldine, 2009). The feasibility of CCS relies on certain requirements: a) it should be cost efficient, b) the storage period should be long enough so that if the CO_2 re-emerges it happens after the peak exploitation of fossil fuels, c) it should have little environmental impact, d) the risk should be minimal, and d) it should not interfere or violate international laws and regulations (Herzog and Golomb, 2004; Gibbins and Chalmers, 2008).

A CCS site can either be subterranean or sub-seabed (Herzog and Golomb, 2004). The potential storage sites are comprised of a vast variety of geological formations such as: deep saline formations, depleted oil and gas reservoirs, unmineable coal reservoirs, or sites that require an enhanced recovery of methane, oil, and gas (Herzog and Golomb, 2004; Metz et al., 2005). Requirements of the storage sites include: depth of at least 1km, and enough pressure to allow a density of about 500kg/m^3; the

storage sites should also have impermeable caps or geological traps that will retain the CO_2 and prevent its seepage towards the surface (Herzog and Golomb, 2004; Metz et al., 2005; Gibbins and Chalmers, 2008).

Naturally, the CCS has associated risks such as the potential seepage of CO_2 from the storage site that consequently releases the stored CO_2 back into the atmosphere or the ocean contributing again to the climate change and ocean acidification (OA) (Metz et al., 2005; Blackford et al., 2009; Yamada et al., 2013). The acidification process can have several effects on the marine biogeochemistry and the marine biota (Blackford et al., 2009; Ries et al., 2009; Yamada et al., 2013). An important highlight is that a leakage event would probably be impossible to stop and it could potentially affect the carbon sink function of the seafloor (Molari et al., 2018).

Since 1972, the popularity of CCS projects has been increasing steadily. There are currently 88 pilot projects around the world and 37 large-scale projects. Indeed, as of 1996 Norway has implemented CCS as a means for CO_2 storage purposes (Fig. 2.1) (Global CCS Institute, 2017). Due to the size of CCS projects and their potential associated risks, it is crucial to study their feasibility and to monitor the on-going CCS projects (Gibbins and Chalmers, 2008). Moreover, it is necessary to assess and study the potential consequences of all the technologies that are going to be implemented in the natural environment. The development of supervising techniques could eventually provide signals for the early detection of CO_2 seepage event in the terrestrial and the marine environment and consequently allow the deployment of mitigation measures (Gibbins and Chalmers, 2008).

Fig. 2.1 Map of large scale CCS projects
Source: (Global CCS Institute, 2017)

2.2 Seawater chemistry

2.2.1 pH and total alkalinity (TA)

pH is a measure of acidity (H^+) of an aqueous solution. The pH is determined by the following equation

$$pH=-Log\{H^+\}$$

Knowing the seawater pH is extremely important because it regulates the inorganic carbon equilibrium in the ocean, nutrients cycles, the marine carbonate saturation, the marine gas exchange between the sea and the atmosphere but also within the ocean, the rate of hydrolysis of the dissolved organic matter and several biogeochemical processes (Dickson, 1993; Prichard and Lawn, 2003; Doney et al., 2009; Ries et al., 2009).

The TA or alkalinity is another important feature of the marine chemistry as it is the buffering capacity found within seawater. The

concentration of dissolved inorganic carbon (DIC) species such as pCO_2, CO_2, HCO_3^-, CO_3^{2-} can be calculated by measuring the TA (Wolf-Gladrow et al., 2007; Reimer and Arp, 2011). The TA is a conservative value and thus it does not change with changes in temperature (T), pressure or mixing (Wolf- Gladrow et al., 2007). It is defined by Dickson, (1981) as the number of moles of H^+ equivalent to the excess of proton acceptors (bases) over proton donors (acids) in one kilogram of sample. In other words, the alkalinity is given by the amount of a strong acid required to neutralize 1L of water (Reimer and Arp, 2011).

2.2.2 Solubility pump (inorganic carbon)

The inorganic carbon system is one of the most important factors that controls the pH and subsequently the chemical equilibrium and carbon sequestration capacity of the ocean (Feely, 2004). When CO_2 interacts with sea water it dissolves and reaches an atmosphere- ocean equilibrium in a time-span from months to a year and thus, the concentration of dissolved CO_2 in the sea surface changes proportionally to the concentration of atmospheric CO_2 (Doney et al., 2009; Feely et al., 2009). The equation that shows this interaction is:

$$CO_2\,(g) \leftrightarrow CO_2(aq)$$

Once the CO_2 has been dissolved in the water it rapidly undergoes hydration and forms carbonic acid (H_2CO_3), which then dissociates in one hydrogen ion (H^+) and one bicarbonate HCO_3^-. The H^+ is then free to interact with one carbonate (CO_3^{2-}), and form another bicarbonate (Feely et al., 2009). In natural surface water conditions, 90% the dissolved

inorganic carbon (DIC) is found as HCO_3^-, about 9% as CO_3^{2-}, and only 1% as dissolved $CO_{2\,(aq)}$ and H_2CO_3 (Feely et al., 2009). The reaction is explained in the following equation:

$$CO_{2(aq)} + H_2O \leftrightarrow H_2CO_3 \leftrightarrow H^+ + HCO_3^- \leftrightarrow 2H^+ + CO_3^{2-}$$

The carbonate in the ocean can either be found as calcite or aragonite depending on its crystalline structure. Their formation or dilution of calcium carbonate ($CaCO_3$) depends on their saturation state Ω and it is explained by the following equation:

$$\Omega = IAP/K_{sp}$$

Where IAP is the ionic activity product of Ca and CO_3^{2-}, and K_{sp} the apparent solubility product (Doney et al., 2009). It is worth mentioning that the aragonite is around 50% more soluble than calcite due to differences in their crystalline structures (Mucci, 1983).

In the case of seepage from a CCS site, when CO_2 seeps from the storage site, there is an excess of CO_2 in the water that causes a chemical reaction, like that of OA in the area surrounding the affected zone (Blackford et al., 2009). This reaction alters the seawater pH and as a consequence causes a change in the carbon cycle. Another factor that is important to take into account is that the solubility of the CO_2 increases with decreasing T and increasing pressure, thus the low T and high pressure of the deep ocean can also enhance the uptake of CO_2 from a seepage site and reduce the buffering capacity of the seawater (Williams and Follows, 2011; Molari et al.,2018).

The OA process of the seawater either globally or locally (i.e. associated to CCS seepage) is known to cause not only a decrease in pH but it may have an impact on various biogeochemical processes, such as increase primary production (Doney et al., 2009; Piontek et al., 2013), enhancement of extracellular enzymatic activity (Piontek et al., 2013), nitrification (Beman et al., 2011), affect the biogeochemistry of trace metals (Hoffmann et al., 2012), induce the production of transparent exopolymer particles (TEP) (Yamada et al., 2013), reduce the biodiversity in oceanic and benthic ecosystems (Blackford et al., 2009; Molari et al., 2018), affect the marine animals signalling molecules (Roggatz et al., 2016), affect the microbial carbon pump (MCP) assimilation and degradation of organic carbon (Piontek et al., 2013), induce changes in the biological communities structure as well as the fitness of the individuals (OCB, 2009; Ries et al., 2009), alter the food web ability to transfer and remineralize carbon (Molari et al., 2018), and eventually affect the long term storage of marine organic carbon (Jiao et al., 2010).

Studying the effects of a seepage event from a CCS site and recreating the environmental conditions of the seabed poses some technical difficulties. This helps to explain why a lot of research regarding the consequences that a low pH event has on the marine biochemistry have focused on experiments at one atm (Engel et al., 2004a; Piontek et al., 2013; Riebesell et al., 2013; Yamada et al., 2013; MacGilchrist et al., 2014; James et al., 2017).

2.2.3 Marine Organic carbon (OC)

The marine OC found in the seawater varies in its distribution depending on space, depth, and time (Gordon, 1971). The OC is classified according

to its size in either: total, particulate or dissolved. The total organic carbon (TOC) is the sum of the particulate and dissolved OC. The particulate organic carbon (POC) is composed of all the particles that are bigger than 0.8µm, in other words all those particles retained by a filter with a 0.8µm pore membrane (Sharp, 1973). The dissolved organic carbon (DOC) is everything that passes through that membrane. It is between 0.001µm and 0.8µm in size (Sharp, 1973). In sea water, the DOC fraction is between 95-98% of the TOC (Sharp, 1973). And the POC fraction concentration is so low that reaches the detection limit of analytical techniques (Gordon, 1971).

Dissolved Organic Carbon (DOC)

The DOC in the oceans is mainly composed of a mixture of molecules and biochemicals derived from detritus, photosynthetic and heterotrophic activity in the photic zone, and planktonic exudates that are transported by convection, circulation, and mixing (Carlson et al., 1985; Williams and Follows, 2011; Hansell, 2013; Yamada et al., 2013; Jørgensen et al., 2014). The DOC is the largest pool of fixed organic carbon in the ocean (Ogawa and Tanoue, 2003). It plays an important role in the global oceanography due to its varied interactions with chemical, biological and physical processes (Ogawa and Tanoue, 2003).

Species of DOC: Labile and Recalcitrant

The DOC molecules have been divided into two different groups: the labile which is defined as the group of DOC that can be consumed or rapidly decomposed by heterotrophic bacteria in a timespan of hours to up to two weeks and therefore, does not accumulate; and the refractory or recalcitrant that is composed of DOC products that are resistant to decay

and microbial utilization, is nutrient poor, and can accumulate (Carlson et al., 1985; Brophy and Carlson, 1989; Søndergaard and Middelboe, 1995; Libes, 2009; Hansell, 2013; Jørgensen et al., 2014). Due to the differences in reactivity and lifetimes (time span over which the concentration of the DOC fraction reaches 1/*e* of its initial concentration) of DOC within different groups, five fractions have been proposed and described by Hansell (2013):

- Labile DOC (LDOC): Lifetime of ~10 hours, does not accumulate and has a short presence ranging from hours to a number of days. It is derived from photosynthetic and grazing activity as well as from vertical export and it provides support to the microbial carbon pump (MCP) in the euphotic zone. Its remineralisation products stay in the upper ocean and are exchanged with the atmosphere.
- Semi-Labile DOC (SLDOC): Lifetime of ~1.5 years, presents seasonal variability and is the most important DOC source to the biological carbon pump with a vertical export of ~1.5 Pg C $year^{-1}$. It also supports the MCP in the mesopelagic zone and its remineralisation products reach the air/sea interface in a matter of months to years.
- Semi-Refractory DOC (SRDOC): Lifetime of ~20 years, is potentially important for carbon sequestration. It reaches great depths in the North Atlantic, and is also of secondary importance to the MCP, with a production rate of ~0.34 Pg C $year^{-1}$. Its remineralisation products reach the sea/water interface from decades to centuries.

- Refractory DOC (RDOC): Lifetime of ~16,000 years. It is the biggest pool of exchangeable carbon in the Earth´s surface and is present in every ocean. It is relevant in the climate time-scale; the carbon reaches the air/sea interface over centuries to millennia and thus, can be a key influence in the climate. It has a minor contribution in the carbon export with ~0.043 Pg C $year^{-1}$ and has a great radiocarbon age of at least 4,000- 6,000 years.
- Ultra-Refractory DOC (URDOC): Lifetime of ~40,000 years. This is the least observed and understood fraction; it is the transition of carbon from the biological to the geological realm. Some of its components include polycyclic aromatic molecules found in sedimentary fossils, also known as thermogenic black carbon.

On average, the DOC goes through a yearly rapid cycle of removal and release from the surface layer and into the deep water and vice-versa; this cycle comprises about 1.9 Pg $year^{-1}$ (Jiao et al., 2010; Hansell, 2013). Besides the different fractions, the different sizes of DOC are also important being the low molecular weight (LMW) molecules (<1KDa) the most abundant in the water column with approximately 65 – 80% of the bulk DOC whereas the high molecular weight molecules (HMW) account for 20-35% when the molecules are >1 KDa and 2-7% for molecules >10 KDa and is primary composed of polysaccarides (Ogawa and Tanoue, 2003; Engel et al., 2004a).

Origin of DOC

The newly produced DOC is generally derived either from the primary producers extracellular releases such as mucilage sheaths and capsules; from grazing activities such as sloppy feeding or from cellular lysis due

to senescence, viral attacks or predation (Nalewajko, 1977; Søndergaard and Middelboe, 1995; Libes, 2009; Jiao et al., 2010; Hansell, 2013). The molecules released by the primary producers are a mixture of amino acids, proteins, sugars, carbohydrates and lipids (Carlson et al.,1985; Williams et al.,1986; Jørgensen et al.,2014). The neutral sugars produced by algae are apparently more labile than those produced by bacterial decomposition and as a consequence, more easily transformed from labile to recalcitrant forms (Jørgensen et al., 2014).

Some molecules escape the rapid remineralization of the newly produced LDOC, this remaining LDOC can then be transformed by the enzymes of heterotrophic bacteria (Piontek et al., 2013). When the bacterial community utilizes HMW molecules or POC as a source for an organic substrate, the heterotrophic bacteria produce hydrolytic enzymes that turn the HMW molecules into LMW molecules that can be easily taken up (Amon and Benner, 1996; Ogawa and Tanoue, 2003; Piontek et al., 2013).

The release of enzymes also contributes to the RDOC pool (Jiao et al., 2010). The uptake LDOC is fast and occurs in hours to days; the transformed products can persist in the water over extended periods of time from months to millennia (Iturriaga and Zsolnay, 1981; Brophy and Carlson, 1989; Ogawa, 2001). It is important to note that the molecules that are recalcitrant to one group of organisms could be labile to another group (Hansell, 2013).

Jiao et al.,(2010) explains that the MCP has two main implications, the first is the build up of a recalcitrant carbon reservoir for the long-term carbon storage; and the second, is the chemical change of DOC and the consequent change in the ratios of several elements such as

nitrogen and phosphorous, among others. Moreover, the molecular composition of the neutral sugars in seawater is determined by the bacterially produced neutral sugars from the degradation process (Jørgensen et al., 2014).

As noted before, the carbon pump and the MCP are closely related and thus, it is essential to study what could happen to the marine carbon chemistry under low pH exposure as well as with the marine bacterial community that transforms the LDOC and RDOC, as in the long term, the changes that occur in the marine chemistry will have worldwide implications in the climate, biodiversity, food webs, and the carbon cycle regulation (Orr et al., 2005; Piontek et al., 2013).

Mechanisms of DOC fractions transformation and removal

The DOC in the oceans is removed by both biotic and abiotic processes (Brophy and Carlson, 1989; Hansell, 2013). The biotic processes involve the transformation of the consumed LDOC and SLDOC into more recalcitrant species by the MCP and are of greater importance than the abiotic processes (Brophy and Carlson, 1989; Hansell, 2013).

The abiotic removal can happen in different ways: photochemical radiation and UV light can transform LDOC into RDOC (Libes, 2009). In other instances, the photolysis of RDOC molecules can transform them into LMW LDOC molecules ready for microbial remineralization and respiration (Mopper et al., 1991; Ogawa and Tanoue, 2003; Hansell, 2013). However, UV photolysis is not relevant for the DOC gradients of the deep sea (Hansell, 2013).

The RDOC removal can also happen due to the accretion of LMW molecules into HMW molecules and the subsequent aggregation or

binding of polysaccharide particles into gels or TEP that are eventually big enough to be sinking particles as marine snow (Nalewajko, 1977; Carlson et al., 1985; Engel et al., 2004b; Jiao et al., 2010). The TEPs are rich in carbon and poor in nitrogen; their aggregation is relevant for the DOC gradient found in the deep ocean because it amplifies and accelerates the gravitational export of carbon into the deep sea increasing the total particulate volume in the seawater (Carlson et al., 1985; Engel et al., 2004b, 2004a, 2014; Hansell, 2013; MacGilchrist et al., 2014). The sinking polysaccharides also act as a control for trace metals residence times in the surface ocean due to their strong binding sites that cause the aggregation and eventual sedimentation of trace metals (Engel et al., 2004b). Moreover, the TEPs act as a substrate for bacterial growth and thus, a higher concentration of TEPs could positively affect the bacterial community (Engel et al., 2014).

In order to understand the fate of amino acids in the ocean the change in the ratio of D/L amino acids should be studied once the molecules have been transformed following the process of microbial degradation (Jørgensen et al., 2014). Dissolved protein has a degradation rate in seawater similar to that of monomeric amino acid turnover and it is faster than the respiration of transformed HMW molecules (Brophy and Carlson, 1989).

The binding of molecules that are less hydrophobic such as glucose or glycine show that other mechanisms like metal bridging via magnesium (Mg) or calcium (Ca), ester formation, hydrogen (H) bonding and the Maillard reaction may also play an important role in the formation of HMW molecules in seawater (Carlson et al., 1985).

DOC distribution in the oceans

One of the interesting aspects of the DOC composition in the oceans is that regardless of the location, the molecules initial origin, or the bacterial community that degrades it, the refractory neutral sugars have a similar composition in the seawater (Jørgensen et al., 2014). In the surface waters the concentration of DOC ranges from 60 – 80μM excluding the Antarctic Ocean and the deep waters (Ogawa and Tanoue, 2003). And globally the carbon stock of bulk DOC is of approximately 700Gt with 650Gt belonging to RDOC and 50Gt to LDOC (Ogawa and Tanoue, 2003).

As the ocean acts as a carbon sink, it is important to address the role of the refractory fractions in the long-term storage of carbon in the ocean. The average radiocarbon age of RDOC and URDOC is higher than the thermohaline circulation turnover time (~1000 years) (Ogawa and Tanoue, 2003). This makes them specially important for the removal of carbon from the atmosphere as they remain fixed in the seawater (Ogawa and Tanoue, 2003). It is for this reason that the bacterial decomposition processes in the MCP that produce RDOC become relevant for the carbon cycle and global climate regulation (Jiao et al., 2010; Hansell, 2013).

The degradation of POC is also one of the main factors that influences the composition of DOC in the deep ocean (Jørgensen et al., 2014). Regarding the contribution of the marine snow and the total amount of DIC and DOC in the deep ocean, the rain is regulated by the ratio or proportion of organic carbon to inorganic carbon that sinks into the ocean that is in average a ratio of 5:1 (Williams and Follows, 2011).

2.3 Biological carbon pump (BCP)

The BCP is defined as the processes involved in the transformation and integration of inorganic carbon into organic carbon structures (Ducklow et al., 2001). The transformation is mediated by photosynthetic activity of the primary producers, food web structure and incorporation of carbon as part of the organisms biomass (Ducklow et al., 2001). Following the incorporation, the produced DOC or POC is pumped into the deep ocean in the form of faecal pellets or sinking particles (Ducklow et al., 2001).

2.3.1 Microbial carbon pump (MCP)

The MCP plays a key role regarding the DOC transformation from labile to recalcitrant forms (Jiao et al., 2010). However, it is important to differentiate the microbial carbon loop (MCL) from the MCP. The MCL is the microbial food chain that happens between bacteria, archaea, virus, metazoans, and protists whereas the MCP is the production of recalcitrant DOC by the microbes in the ocean (Jiao et al., 2010).

The MCP is responsible for about 23% of the total DOC pool and it accounts for the key role that microbial mechanisms play when transforming labile DOC into recalcitrant DOC and the eventual contribution of the RDOC to the long-term storage of carbon in the ocean (Nalewajko, 1977; Saunders, 1977; Ogawa, 2001; Ogawa and Tanoue, 2003; Jiao et al., 2010; Hansell, 2013; Jørgensen et al., 2014). The cell surfaces of marine microbes account for most of the biotic surface area in the ocean, and their diversity of cell surfaces could be an important contributor to the marine RDOC (Jiao et al., 2010).

Bacteria are particularly resilient organisms and are the main agents that use dissolved organic molecules with high efficiency (Nalewajko, 1977; Saunders, 1977; Iturriaga and Zsolnay, 1981). Ocean

raising T and an elevation of pCO_2 are expected to increase bacterial activity and affect their capacity to transform DOC; the environmental changes are expected to cause a stronger stratification of the ocean leading to oligotrophic areas and enhanced DOC transformation (Jiao et al., 2010). The changes on the bacterial influence on the carbon flow system and the DOC composition in the seawater make the MCP relevant to long-term carbon storage (Jiao et al., 2010).

2.4 Effect of high CO_2 on the DOC and the bacterial community

The study of the effects of low pH on the DOC on the bacterial transformation of DOC is a fairly new realm of study (Zark et al., 2015). However, it is already known that low pH affects the DOC (Zark et al., 2015).

Earlier reports about the effects of high pCO_2 on the primary producers are not necessarily consistent in their findings. On the one hand, the increased uptake and transformation of carbon into organic carbon under high pCO_2 conditions is expected to increase the photosynthetic activity of the primary producers and as a consequence, increase the amount of extracellular releases (ER) and LDOC thus affecting the remineralization rates of the microbiota (Engel et al., 2004a, 2014). This effect has also been seen when there is a shortage of inorganic nutrients (Riebesell et al., 2013). On the other hand, it has been reported that a higher concentration of CO_2 does not affect the production of DOC from the primary producers (Engel et al., 2004a).

The bacterial activities are also affected by the changes in the pCO_2 (Grossart et al., 2006; James et al., 2017). Regarding the bacterial

activity it has been reported that the pH strongly affects biochemical processes of the marine bacteria such as the respiration and electron transfer, enzymatic reactions, production of extracellular hydrolytic enzymes, and nitrogen fixation (Kolber, 2007; Piontek et al., 2010, 2013; Borrero-Santiago et al., 2017). When the microbiota is exposed to changes in their environment they respond rapidly in one of the following three different ways as mentioned by Saunders (1977):

1. Passive response.- the change is controlled by the environment and the organisms change to a new state as response to the environmental changes
2. Regulative response.- the changes observed are related to the inability of the organisms to keep their constancy
3. Controlled response.- the organisms adapt their changes in a controlled matter until they reach a new state

Experiments studying the effects that a lower pH would have in the bacterial community show contrasting results. In some studies the high pCO_2 is negatively affecting the bacterial community diversity (James et al., 2017) and the bacterial growth and cell number (Borrero-Santiago et al., 2016). In other cases it has been reported that the low pH conditions are positively affecting the bacterial activity (Grossart et al., 2006; James et al., 2017), abundance (Zark et al., 2015), hydrolytic enzymatic activities and rates of incorporation of carbon as bacterial biomass (Piontek et al., 2013), respiration (James et al., 2017), as well as increasing the production of DOC (Yamada et al., 2013). In addition, it has been suggested that the low pH is not directly affecting the metabolism and physiology of marine bacteria but the activity of the released enzymes due to a higher concentration of H^+ that interact with

the enzymes under high pCO_2 conditions (Piontek et al., 2013; James et al., 2017). Moreover, the higher amount of DOC consumption is not converted to bacterial biomass but respired as CO_2 (James et al., 2017).

An elevated pCO_2 increases primary production and as a consequence, the concentration of organic matter increases (Piontek et al., 2013). However, under low pH there is also an increase in bacterial enzymatic activity that enhances the degradation and hydrolysis of DOC (Piontek et al., 2013; James et al., 2017). The bacterial community is capable of degrading the enhanced production of organic matter in the surface ocean (Piontek et al., 2013; Zark et al., 2015; James et al., 2017). The increased bacterial respiration of the LDOC in the surface could decrease the amount of carbon available for export into deeper waters and it can increase the outgassing of CO_2 into the atmosphere (James et al., 2017). Contrastingly, it has reported that there are no changes in the rate of bacterial decomposition of organic matter regardless of the pCO_2 values (Yamada et al., 2013) neither on the RDOC species (Zark et al., 2015). It is important to mention that in cases where there is an increased production of DOC under low inorganic nutrients - high CO_2 conditions the bacteria are limited by the lack of nutrients and are not stimulated by the higher amount of available DOC (Riebesell et al., 2013).

In addition, the acidification of seawater promotes the aggregation of TEP´s and results in an enhanced coagulation of suspended particles and eventually, a higher rate of carbon transfer via sinking of organic carbon from the surface to the bottom of the water column (Engel et al., 2004a, 2014; Yamada et al., 2013). Engel et al. (2004a) reported that there is a positive correlation between a higher concentration of CO_2, a higher primary production, and a greater production of TEPs. The POC

concentration will be positively affected by a higher production of ER and aggregation of TEPs (Engel et al., 2014). Contrastingly, MacGilchrist et al. (2014) reported that a higher pCO_2 does not show a positive relationship with a higher production of TEPs.

2.5 DOC characterization (DOC/C)

Low pH induced changes on the bacterioplankton consumption of DOC and the molecular composition of marine DOC can have consequences in its reactivity, long-term accumulation and global marine carbon inventories (Zark et al., 2015; James et al., 2017). Therefore it is important to study how the marine carbon pool behave under high pCO_2 conditions and how the different labile and recalcitrant species affected.

The characterization of DOC is still a fairly unknown realm with <10% of the surface ocean DOC molecules and <5% of the deep sea DOC molecules being chemically and structurally characterized, and thousands of mass formulas identified (Libes, 2009; Jiao et al., 2010). Some of the difficulties are that the concentration of DOC in the seawater is below the detection limit of some of the characterization techniques and that there is a high amount of salts (Brophy and Carlson, ; Dittmar et al., 2008). Another drawback is that it is not yet understood how a normal heterotrophic process can uptake LDOC and produce molecules that can no longer be utilized as a by-product (Brophy and Carlson, 1989). However, it is known that DOC tends to move from a more available to a less biologically available form (Brophy and Carlson, 1989).

There are two main ideas of what could be the principal component of RDOC in the ocean. On the one hand, it is though that LMW DOC is transformed into HMW products and that these products are resistant to bacterial degradation and thus, can persist for longer

periods of time (Brophy and Carlson, 1989). On the other hand, it has been proposed that due to the higher amount of LMW molecules in the water column (65-80%) the HMW molecules should be the reactive fraction, and the LMW molecules the refractory fraction (Ogawa and Tanoue, 2003).

Most of the molecules that have been characterized are carbohydrates and molecules of <1 k Da; the second largest class is amino sugars (Ogawa and Tanoue, 2003; Libes, 2009). Some of the LMW molecules that have been characterized are glucose, cellulose, alginic acid, leucine, chitin, palmitic acid, alanine, valine, glycine, arginine and glutamic acid (Iturriaga and Zsolnay, 1981; Carlson et al., 1985; Brophy and Carlson, 1989; Ogawa and Tanoue, 2003; Libes, 2009). In addition, the biggest pool of characterized components in the deep ocean is comprised of refractory carboxyl-rich alicyclic molecules (CRAM) (Hertkorn et al., 2006).

3 Justification

The current increase of CO_2 in the atmosphere is affecting the marine chemistry by lowering the seawater pH and as a consequence the marine carbon cycle (Feely et al., 2009). The CCS has been proposed as a way of managing the raising concentration of CO_2 in the atmosphere (Gibbins and Chalmers, 2008). However, seepage from an underwater CCS site would cause a drop in the seawater pH similar to that of OA (Blackford et al., 2009). As a consequence of this, the organic matter cycling as well as the sinking flux of carbon in the ocean can be affected (Grossart et al., 2006).

Current studies on DOC and OA have focused on experiments at 1atm of pressure (Engel et al., 2004a; Piontek et al., 2013; Riebesell et al., 2013; Yamada et al., 2013; MacGilchrist et al., 2014; Zark et al., 2015; James et al., 2017; Molari et al., 2018). However, none of them has addressed the deep-sea environmental conditions that are characteristic of sub-seabed CCS site. The novelty of the study presented in this thesis is that we studied the long-term effects of OA due to the possible CO_2 seepage on the different species of organic carbon, the DOC/C and the bacterial production of DOC. The knowledge obtained from this study would allow for the creation of scenarios and models that address the effect of OA and seepage from a CCS facing high pressure of the deep-ocean and long-term low pH exposure.

4 Hypothesis

An increase of pCO_2 caused by a high concentration of CO_2 in the seawater provokes a decrease in the seawater pH. The hypothesis is that the high-pressure and low pH conditions will affect the different species of marine organic carbon as well as the characterization of the DOC. We also hypothesize that the long-term low-pH conditions will affect the bacterial community and as a consequence, their DOC degradation.

Moreover, it is important to study how the process of acidification and its consequences would occur in the deep ocean and the area surrounding the storage site. In this thesis the Karl Erik pressurised Titanium Tank (TiTank) was used in order to evaluate the potential changes experienced by the different organic carbon fractions, the DOC species, and the bacterial degradation of DOC under high-pressure low pH.

5 Objective

The main objective is to investigate the possible effects that long-term, high-pressure, low pH conditions derived from a potential leakage of CO_2 from a CCS site would have on the particulate and dissolved marine organic carbon and on the bacterial decomposition of DOC. This will include the following elements:

- Study how the POC and DOC concentration changes over time
- Study how the POC and DOC concentration changes after bacterial decomposition in order to evaluate the impacts of low pH on the bacterial community
- Characterize and compare the DOC found in different treatments
- Characterize DOC after bacterial decomposition and search for differences before and after low pH stress

6 Materials and methods

6.1 CO_2Marine project

The CO_2Marine project is a project of the University of Gdańsk under the collaboration with the Medical University of Gdańsk, the Norwegian University of Science and Technology, Stiftelsen Sintef, and the Norwegian Institute for Water Research. The project aimed to address the environmental risk assessment related to the seepage of CO_2 from a projected sub-seabed CCS storage site in the polish Baltic Sea (B3 field) (University of Gdansk, 2013). The Baltic sea is a brackish water sea and thus has a lower salinity (S) than the open ocean, this reduces its alkalinity and its buffering capacity to an acidification event (Piontek et al., 2013). The objective of the project was to study the effects that a CO_2 seepage event and the subsequent drop in pH would have in the sediment, seawater, trace elements, two benthic species (*Hediste diversicolor* and *Limecola Baltica*), and in the microbiology, in order to determine the biomarkers that could be used in case of pH stress (University of Gdansk, 2013). The experiment was performed using a hyperbaric titanium tank, the Karl Erik Pressurised Titanium tank (TiTank).

For this thesis project, the focus was on studying the changes that a high-pressure long-term CO_2 seepage event from a CCS site would induce in the seawater OC chemistry. Specifically the effect that low pH would have in the transformation of the different species of OC, the DOC/C and the bacterial production of DOC.

6.2 Experiment set up

The TiTank was maintained at a T of 10 °C and a pressure of approximately 9 bar. These conditions were similar to those of the prospected CCS storage site in the Baltic Sea (University of Gdansk, 2013). An image of the TiTank and the carrousel is shown in Fig. 6.1. The scheme of the TiTank water inlet and outlet as well as the samples taken is shown in Fig. 6.2.

The TiTank had a constant flow rate of 0.452 L/min of artificial brackish seawater getting into the tank. The artificial seawater resembled the S and TA of the Baltic Sea seawater. The artificial seawater was prepared by mixing water from Trondheim´s fjord (~33 of S) and fresh water until a S of 7 was reached. The water from the fjord was taken from 80 m depth. The hydraulic retention time of the tank was 37.07 hours. The alkalinity was adjusted by adding a freshwater solution of $NaHCO_3$ (0.095 M) and HCl (0.013 M) at a rate of 3.2 mL/min. The artificial seawater was stored in a tank (blue tank) Fig. 6.2. After the water was prepared, a mixture of fresh algae was also added. The species *Dunaliella tertiolecta*, *Rhodomonas baltica*, and *Isochrysis galbana* (1:2:4) were added with a rate of 3.5 mL/min; the algae were a food source for the animals used inside the TiTank. The TiTank had complete darkness at all times and thus no primary production happened inside it.

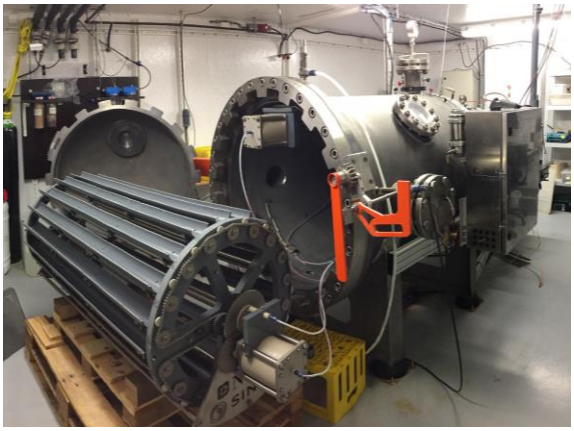

Fig. 6.1 Open TiTank and carrousel without trays
Image: Sara Miquel

The TiTank contained a carrousel with sediment trays Fig. 6.1. The trays were divided in three different groups; each group was filled with a different type of filling. Three different types of filling were used: only sediment, sediment with the polychaete *Hediste diversicolor*, and sediment with the clam *Limecola balthica*. The sediments and animals were collected from the southern Baltic Sea. The sampling of sediment and animals for the control experiment was done on the 4th of January 2017; and the sediment and animal sampling for the pH 7 experiment was done on the 20th October 2016.

The sediments were collected with a Van Veen grab and were not sieved. The well-oxygenated upper layer of 3cm was separated and placed in a separate container. The sub-surface black clay sediments were placed into a different container. The sediments of each container were homogenized prior to distribution into the TiTank trays.

The clams *Limecola balthica* were collected using a sledge dredge. The clams were dragged out, rinsed and collected by hand. Specimens with a size range of 11.44 - 15.00 mm size were selected for

the experiment. The polychaete *Hediste diversicolor* was collected by hand using a Van Veen grab; the polychaetes were collected in the mouth of the Vistula River.

Each tray was filled with a layer of subsurface sediment and a layer of surface sediment; placing the subsurface sediment first and the surface sediment on top. The trays were left to stabilize submerged in a container with running artificial seawater for 24 h. After the sediment stabilization period, the animals were placed in the trays with sediment; they burrowed themselves soon after being placed onto the sediment. The trays with *Hediste Diversicolor* had a plastic net covering them in order to prevent the polychaetes from escaping. In order to evaluate the differences between the sediment trays with nets and without nets, some trays without animals were also covered with nets. All trays were loaded into the TiTank carousel. The TiTank was closed after loading and was not opened until the experiment was finished.

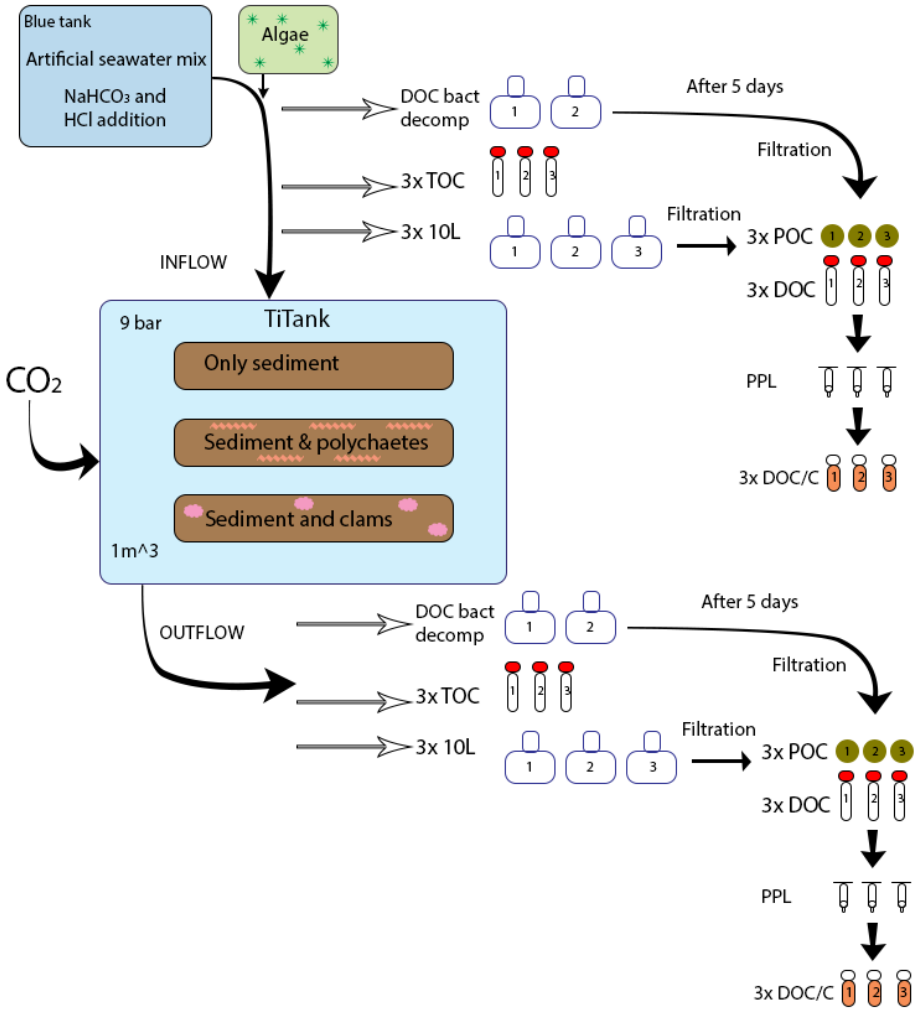

Fig. 6.2 Scheme of the TiTank and samples taken
The artificial brackish seawater mix with $NaHCO_3$ (0.095 M) and HCl (0.013 M) is represented with the blue tank. The algae addition is represented with the green square. The TiTank was held under a 9 bar pressure and had a capacity of 1 m^3. The tank was filled with sediment trays (brown) and water from the blue tank. Samples were taken both from the inflow and the outflow hoses. A scheme of the different samples taken is shown. TOC: total organic carbon, POC: particulate organic carbon, DOC: dissolved organic carbon, DOC/C: dissolved organic carbon characterization, DOC bact decomp: dissolved organic carbon bacterial decomposition. The numbers 1, 2, and, 3 represent each one of the triplicates. Regarding the DOC bacterial decomposition samples, only two samples (duplicate) were taken from the inflow and outflow thus, only 2 replicates of the DOC, POC and DOC/C were taken from the bacterial decomposition experiment.

6.2.1 Sampling plan

Two experiments of 50 days were performed, a control (pH: 7.7) and an experiment under low pH (pH: 7). The frequency of the samplings for both experiments was planed in order to follow the stabilization period detect the initial rapid changes and eventual stabilization of the OC and the bacterial degradation of the DOC. Each experiment had an acclimatization period (ten days) and an experimental period. There were two starting days of the experimental period (day 11^{th} and 12^{th}). In the pH 7 experiment the injection of CO_2 started on day 11^{th} and 12^{th}.

Both experiments had the same water mixture, algae, sediment, animals, and chemical and physical parameters with an exception of the pH and Redox potential. The pH, redox potential, and T of the outflow of the TiTank were measured with Mettler Toledo combination pH redox sensor (Mettler Toledo, PT4805-DXK-S8/120) coupled with a Mettler Toledo M300 transmitter. The dissolved oxygen (DO) was measured with an oxygen meter (Hach LDO-HQ20 Portable Oxygen Meter). The S was measured with a Thermo Scientific Orion 5 star multifunction meter coupled with a conductivity sensor (Thermo Scientific, 013025MD). In the control experiment the pH inside the TiTank was held at 7.7 units with a pCO_2 of 1081 µatm. In the pH 7 experiment the pCO_2 was 4764 µatm.

Control experiment (pH: 7.7)

The control experiment was conducted from January 13^{th} 2017 to March 6^{th} 2017 (Table 6.1). The pH was sustained at pH= 7.7 throughout the experiment.

Table 6.1 Control experiment sampling schedule and samples taken per day

Date	20/01/17	25/01/17	3/02/17	13/02/17	23/02/17	01/03/17	06/03/17
Day of exp	8	13	21	31	41	47	53
TOC	X		X	X	X	X	
DOC	X		X	X	X	X	
POC	X		X	X	X	X	
DOC/C	X			X		X	
Pre BD	X					X	
Post BD		X					X

The red line represents the day of addition of CO_2 of the pH 7 experiment; it is merely used for comparative purposes. Day of exp: day of experiment, BD: bacterial decomposition

CO2 seepage experiment (pH: 7.0)

The pH 7 experiment was conducted from November 2nd 2016 until December 22nd 2016 (Table 6.2). The dosing of CO_2 started on November 11th; the CO_2 dosing rate was 0.3 g/h and the flow rate of the seawater 0.452 L/min.

Table 6.2 pH 7 experiment sampling schedule and samples taken per day

Date	10/11/16	13/11/16	15/11/16	16/11/16	30/11/16	5/12/16	14/12/16	18/12/16	19/12/16
Day exp	9	12	14	15	29	34	43	47	48
TOC	X	X		X	X		X	X	
DOC	X	X		X	X		X	X	
POC	X	X		X	X		X	X	
DOC /C	X	X		X	X			X	
Pre BD	X				X		X		
Post BD			X			X			X

The red line marks the beginning of the addition of CO_2. Day of exp: day of experiment, BD: bacterial decomposition

6.3 OC determination and characterization

Water samples were taken in triplicates for each of the OC samples (TOC, DOC, POC, and DOC/C): three from the inflow and three from the outflow of the TiTank. The inflow water samples were taken from a hose that brought artificial seawater and algae into the TiTank (Fig. 6.2). The outflow samples were taken from a hose that exited the TiTank. Fig. 6.2 shows the TiTank scheme and the samples taken from both the inflow and the outflow.

6.3.1 Cleaning procedure for glass vials and plastic caps

The 40ml vials used for the sample collection of TOC and DOC were cleaned as follows:

1. Remove paper, plastic, or marker labels from all vials
2. Immerse the vials in a HCl 30% bath for at least eight hours
3. Rinse the vials three times with MiliQ water
4. Dry the vials in a drier until completely dry, usually around two hours at 80°C
5. Wrap the vials with aluminium paper in packages small enough to be placed inside a combustion oven
6. Combust the vials in an oven at 450°C for eight hours

The plastic caps of the vials were cleaned separately with the following procedure:

1. Place the caps in a HCl 30% bath for about ten minutes
2. Transfer the caps into a methanol bath (do not rinse after the HCl bath with MiliQ water to avoid contamination)
3. Leave the caps in the methanol bath from six to eight hours

4. Take the caps out of the methanol bath and place them in a semi-closed (to allow evaporation) aluminium foil foiled container
5. Place the caps to dry in a drier at 60°C for two hours or until completely dry
6. Transfer the caps to a plastic bag and keep them sealed until needed

* Gloves, goggles, and lab coat were used at all times; the cleaning was done under a fume hood when needed.

6.3.2 Water collection method

TOC

The TOC samples were taken directly from the inflow and outflow hoses using 40 ml pre-combusted vials (QEC 2112-40mlE). The vials were rinsed three times with sample water and then filled to ¾ of their capacity. The TOC vials were stored in a freezer at -20°C.

POC and DOC

A total volume of 4.5 L of water was collected in triplicates from both the inflow and the outflow for the POC and DOC samples. The samples were collected using 10 L pre-acid washed flat bottom flasks; each flask was rinsed three times with sample water before sample collection and then filled to a little over half their capacity. The water collection is shown in Fig. 6.3.

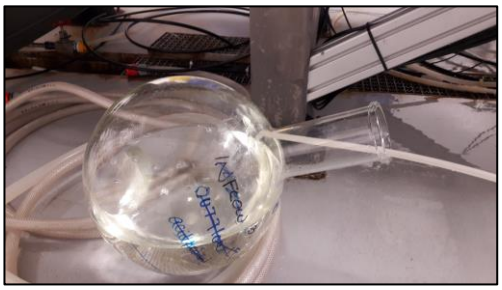

Fig. 6.3 Water collection from the outflow hose from the TiTank into a flat bottom flask
Approximately 4.5 L were collected for the DOC, POC and DOC/C sampling.

POC

A total volume of 4.5 L in each replicate was filtered with glass fibre filters GF/F 0.7 µm (Whatman, 1825-047) utilizing a vacuum filtration system with a 250 ml filter holder (Sartorius, filter holder 16309) and a Büchner Flask (Fig. 6.4). The filtration of each triplicate was performed in two batches due to the volume limitations of the 2 L Büchner flask.

Two GF/F filters were used for each triplicate because of the filters clogging (Fig. 6.5). When the first 2000 ml were filtered they were transferred to a new, pre-rinsed (with filtered water) flat bottom flask and the GF/F filter was folded and wrapped in aluminium paper, labelled and stored in a plastic bag. After the filtration of the first 2000 ml, another new GF/F filter was put in the filtration system and 2200 ml were filtered and transferred to the 10 L flask that already contained the first 2000 ml of filtered sample; the second filter was also labelled and stored. The extra 200 ml were taken to counteract any water volume loses due to the rinsing of the 10 L flask, the rinsing of the 40 ml vial, and the sampling of DOC. The final volume of filtered seawater was standardized to 4000 ml. The POC filters were stored in a freezer at -80°C.

Fig. 6.4 Filtration of water for DOC and POC sampling
The filtered water was transferred to a new, clean flat bottom flask (right) and that filtered water was used for the DOCC sampling.

.

Fig. 6.5 POC filters after the seawater filtration

DOC

The DOC samples were taken after the collected seawater was filtered. The sample was taken in a 40 ml pre-rinsed (3x with filtered water) glass vial (QEC 2112-40mlE) and filled up to ¾ of its capacity. The DOC vials were stored in a freezer at -20°C.

Bacterial decomposition (BD) Samples

Sample preparation

For the BD experiments duplicates of 10 L of water from the inflow and from the outflow of the TiTank were taken. Each 10 L flat bottom flask was pre-rinsed three times with sample water. The 10 L of seawater were filtered with a precombusted glass microfiber GF/C 1.2 µm filter (Whatman, 1822-047) in order to eliminate grazers, algae, and other particles. The filter was not changed over the 10 L filtration and it was discarded after the filtration was completed. The flasks were wrapped in aluminium foil, sealed with two layers of Parafylm and stored in a dark room at 10 °C for five days to allow heterotrophic and anaerobic decomposition from the bacteria and to bring down to zero the photosynthetic activity of the algae that could have gone through the filtration (Saunders, 1977). The samples were allowed to decompose for five days given that this time-span is more that enough to allow a change in the composition of DOC though the decomposition and transformation of LDOC forms into RDOC forms, as shown in previous experiments (Iturriaga and Zsolnay, 1981; Brophy and Carlson, 1989; Jørgensen et al., 2014; MacGilchrist et al., 2014).

Post BD

After five days of decomposition 4 L from each of the four bottles with 10 L were taken. The four bottles with the remaining ± 6 L of seawater were sealed with Parafylm and brought back to the dark and cold room. The procedure for sampling POC and DOC was the same as that of the seawater samples from the TiTank.

DOC/C

The bottles with 4000 ml of filtered seawater (from the POC and DOC sampling) were used for the DOC/C. The method followed for the extraction of DOC was according to Dittmar et al. (2008). The pre-filtered 4000 ml were acidified with HCl (3 M) to a pH: 2.0. After the addition of the required volume of HCl (3 M), the flasks were mixed in order to homogenize the sample.

After the samples were acidified, the organic compounds were extracted using a solid phase extraction technique (SPE). We used six PPL columns of 500 mg (Agilent, Bond Elut-PPL) one for each flat bottom flask. The PPL columns were pre-rinsed with 6 ml of ultrapure methanol in order to eliminate impurities before placing them inside the sample. The flow rate of the acidified sample through the PPL column was about 2.54 mL/s. The arrangement of the flasks, PPL columns, and the peristaltic pump is shown in Fig. 6.6.

Once the 4000 ml sample had passed through the column, the column was rinsed with 5 ml of HCl (0.01 M) in order to eliminate the salt residue from the resin. After the salt residue removal, the organic compounds were extracted from the column with 5 ml of ultrapure methanol, twice; the columns were put on a support where they were left to drip 10 ml of methanol into a 20 ml glass vial (Fig. 6.7). After extraction, the vials were tightly closed, put in a sealed plastic bag, and stored in ambient T.

Fig. 6.6 Arrangement of solid phase extraction (SPE)
Each PPL column was connected with a plastic tube joint to a pipette that was previously rinsed with methanol; the pipette was linked with a flexible plastic hose to a peristaltic pump. The PPL and glass pipette were placed inside the flat bottom flask. In order to ensure a full seal, Parafylm was used between the pipette and the flexible plastic tube.

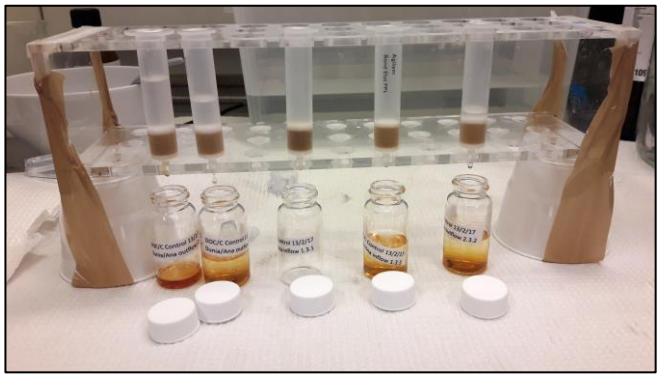

Fig. 6.7 Extraction of organic compounds with methanol from the PPL columns
The extraction was left to drip into the glass vials; no extra force was used in the extraction of the compounds

6.4 Samples analysis

6.4.1 Partial pressure of CO_2 (pCO_2) and total alkalinity (TA)

The calculation of the pCO_2, the DIC species as well as the saturation of calcite and aragonite was done with the software

CO2SYS_MACRO_MAC_PC_2011 (Pierrot et al., 2006). The parameters used were:

Set of constants: K1, K2 from Mehrbach et al. (1973) refit by Dickson and Millero, (1987)

$KHSO_4$: Dickson

pH Scale: Total scale (mol/kg-SW)

The TA was measured by titration of a seawater sample with HCl (0.02 M) (AVS TITRINORM, VWR). The samples were acidified to a pH between 3.4 and 3.9 units. Samples of 50 ml of water from the inflow and from the outflow were analyzed. The pH was measured with a pH sensor (PHM2010, MeterLab).

6.4.2 DOC analysis

The TOC and DOC samples were analyzed by the Norwegian Institute for Water Research with a TOC analyzer Apollo 9000 HS TOC-instrument (Tekmar Dohrman, Serienr. 01061005190B1048). The TOC analyzer works by indirectly measuring the amount of carbon in a sample. The analyzer oxidizes all the organic molecules found in an aliquot of the water sample to CO_2 by combusting the sample (680-1000°C); the sample is gasified and its concentration of CO_2 is measured by a Non-Dispersive Infra-Red (NDIR) detector that is specific for detecting the CO_2 from OC oxidation; the amount of OC is expressed in concentration of carbon in mg C/L (SUEZ, n.d.; Teledyne Tekmar, n.d.). The equipment used for the analysis of the TOC and DOC samples had an accuracy of 80%. The precision and accuracy of the TOC determination were not satisfactory and thus, the TOC data will not be used.

6.4.3 POC analysis

The POC filters were analyzed with an elemental analyzer at the Department of Plant Sciences in the University of California Davis (UC Davis), Stable Isotope Facility, California, USA. The functioning of an elemental analyzer is explained by Verma, (2012); the analyzer works by injecting the sample capsule into a furnace with pure oxygen that combusts it. The resulting oxidized combustion products are carried with a carrier gas (usually an inert gas) into a copper chamber that removes the oxides. After passing through the copper chamber the gases are passed through a water trap that has cells that measure the amount of H, carbon (C) and nitrogen (N) in the sample.

The POC filters were used for two different analyzes: 13C, and bulk C and 15N. For the 13C analysis the filters were defrosted, cut in half and acidified for 40 min with HCl (3 M). Following the acidification, the filters were encapsulated using two tin capsules. The filters chosen for bulk C and 15N analysis were not treated with acid and were only encapsulated using two tin capsules. The filters were analyzed for 13C and/or 15N isotopes using an Elementar Vario Micro Cube elemental analyzer (Elementar Analyzensysteme GmbH, Hanau, Germany) interfaced to an Isoprime VisION isotope ratio - mass spectrometry (IR-MS) (Elementar UK Ltd, Cheadle, UK). Samples were combusted at 1000°C in a reactor packed with chromium oxide and silvered copper oxide. Following combustion, the oxides were removed in a reduction reactor (reduced copper at 650°C). The helium carrier then flowed through a water trap (magnesium perchlorate and phosphorous pentoxide). The CO_2 was retained on an adsorption trap until the N_2 peak

was analyzed; the adsorption trap was then heated releasing the CO_2 to the IR-MS.

During analysis, samples were interspersed with several replicates of at least four different laboratory reference materials. These reference materials had been previously calibrated against international reference materials, including: IAEA-600, USGS-40, USGS-41, USGS-42, USGS-43, USGS-61, USGS-64, and USGS-65 reference materials. A sample's provisional isotope ratio was measured relative to a reference gas peak analyzed with each sample. These provisional values were finalized by correcting the values for the entire batch based on the known values of the included laboratory reference materials. The long-term standard deviation was 0.2 per mil for 13C and 0.3 per mil for 15N (Personal communication with Emily Schick (UC Davis)).

6.4.4 DOC/C analysis

6.4.5 Liquid Chromatography- Mass Spectroscopy (LC-MS)

The characterization of DOC was performed with liquid chromatography- mass spectrometry (LC-MS), this technique was chosen because it gives an overview of all the molecules found in the samples and it can resolve compounds found in DOC on a molecular formula level (Zark et al., 2015). LC-MS is an analytical technique that allows the separation and identification of polar compounds in a liquid sample based on their charge and their mass to charge ratio (m/z) value (Crawford Scientific, n.d.; Peterson, 2016).

As explained by Grumbach et al. (2012) and Peterson, (2016), in the LC-MS analysis the samples are picked up by the sampler, injected and run along with a mobile phase (fluid). The sample is then carried

though a separation column that shifts polarity through the analysis. It is in this separation column where the separation, due to the analytes affinity to the column´s solid phase, occurs. Some analytes will have more affinity for the column and stay longer inside it whereas others will have low affinity and go through it faster, this depends on the solid medium being more hydrophobic or hydrophilic.

In a reversed phase separation, the hydrophobic compounds adsorb onto a hydrophobic solid phase in a polar aqueous phase. However, when a more organic solvent is added, the polarity and hydrophobic interaction decrease causing the hydrophobic analytes to desorb from the solid phase into the mobile phase. After the analytes have been separated inside the column they go through the mass spectrometer. In the mass spectrometer the analytes are ionized by an electric charge and separated depending on their mass to charge (m/z) ratio. It is possible to detect compounds with different charges. In the positive mode analysis only the positively charged ions are detected and in the negative mode, only the negatively charged compounds are detected. The following diagram (Fig. 6.8) shows the LC-MS arrangement.

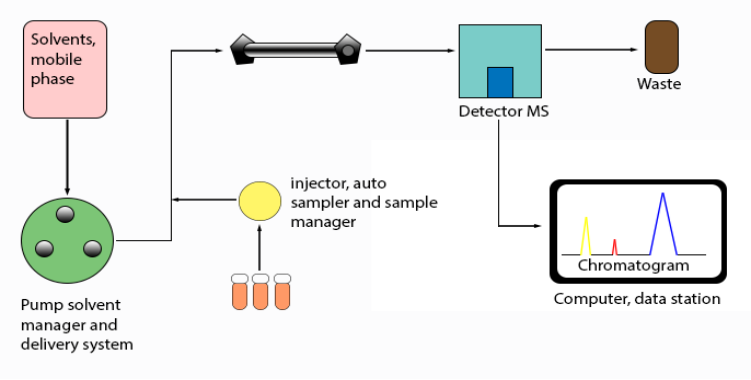

Fig. 6.8 LC-MS diagram design
Adapted from Grumbach et al. (2012)

For this experiment the samples were prepared taking 1ml from each of the SPE extracts from the DOC/C sampling. The 1 ml was transferred to a 1.5 ml chromatography amber vial. The samples were analyzed in the Mass Spectrometry Lab of the Natural Sciences Faculty of the Norwegian University of Science and Technology, Trondheim, Norway (Fig. 6.9).

The Non targeted LCMS-MS analyzes were done on Waters Acquity UPLC connected to Synapt- G2S using ESI as ionization method both in positive and negative mode. Waters HSS T3 100 mm column was used for separation with mobile phases A: Water (w/ 0.,1 % formic acid) and B: Acetonitrile (w/ 0.1 % formic acid). ESI source used a capillary voltage of 3kV. In positive mode, and 2,5kV. in negative mode. Collision energy was ramped from 15-40 eV. Leucine enkephaline (1 ng/ml with a flow of 10 ul per min) was used as lock mass correction. The liquid chromatography gradient was initially at 95% A and 5% B, 0.5 min 95% A and 5% B, 18 min 5% A and 95% B, 1 min 100% B and 2 min 95% A and 5% B with flow rate of 0.300 ml/min. The injection volume was 5µL. The program MassLynx v4.1 SCN871 was used for instrument handling and the program Progenesis QI V2.2. was used for data processing. No standards were used since the aim was to screen all the molecules in the samples (Personal communication with Dr. Susana Villa Gonzalez; Nonlinear Dynamics, 2015).

Fig. 6.9 LC-MS equipment
a) DOC/C samples inside the chromatography amber vials and placed inside the LC-MS spectrometer tray. b) LC-MS spectrometer used for the measurements of the samples.

6.4.6 Nuclear Magnetic Resonance (NMR)

Five samples from the pH 7 experiment DOC/C samples were chosen for Nuclear Magnetic Resonance Spectroscopy (NMR) analysis. The sample preparation for the NMR analysis was done as follows. Five 10 ml test tubes were cleaned following the same procedure previously mentioned for the TOC - DOC vials. After the HCl bath, drying, and combustion of the test tubes, 1 ml of each of the chosen DOC/C samples was added inside each of the test tubes. The samples inside the test tubes were dried with nitrogen in a Biotage TurboVap LV retrofit; the nitrogen air pressure was adjusted to 1 psi or just enough to cause gentle turbulence on the surface of the liquid. The samples were dried for 2:30 hours or until completely dry. After drying they were sealed with parafylm to prevent hydration. The samples were re-suspended with 0.5ml of deuterated methanol (methanol-D4, Sigma-Aldrich, lot number:

MBBC1684), transferred to a 3mm NMR tubes and placed inside the NMR equipment, the samples were analyzed with a Bruker 800 MHz Avance III HD magnet system equipped with a 5-mm cryogenic CP-TCI z-gradient probe and SampleJet. The data from the NMR analysis was not ready to be included in this thesis.

6.5 Data analysis/ statistical analysis

6.5.1 Outliers' calculation for the DOC and POC samples

The outliers of the DOC were calculated by first organizing all the data for each of the OC groups, in other words, all the data of the DOC control, both inflow and outflow together were used in the calculation of outliers. After arranging the data, the first quartile (Q_1), the third quartile (Q_3) and the inter quartile range (IQR) were calculated. After the calculation of these values, the lower and upper range are given by Q_1 - (IQR (1.5)) and Q_3 + (IQR (1.5)), respectively.

The outlier's calculation was done for the samples values of the control DOC and experiment pH 7 DOC. The omission of outliers was only done when the data belonged to a sample that had been transferred to a new vial due to the damage of the first vial. If the values were outside that range but belonged to an uncorrupted vial, the value was accepted. This decision was taken in order to eliminate the influence of possible contamination during the transferring process.

6.5.2 Delta value

The delta value (Δ) is the difference or change between two values of a certain variable. In this case, we calculated the Δ to see the difference

between inflows and outflows as well as between pre and post decomposition samples. Δ is given by the following equation:

$$\Delta x = x_2 - x_1$$

A negative Δ shows that x_1 is greater than x_2; a positive Δ indicates a greater value for x_1 with respect to x_1.

6.5.3 DOC/C LC-MS data analysis

The analysis of the data obtained from the LC-MS analysis was analyzed with the software Progenesis QI V2.2. The data treatment consisted of several steps:

1. Import of data from the program MassLynx v4.1 SCN871
2. Review alignment
3. Experiment set up.- in this step the user can decide whether to use a between-subject or within-subject design, it depends on the kind of analysis that best fits the data. For this experiment the analysis between-subjects was chosen.
4. Peak picking.- in this section the user chooses the data to be included in the peak picking analysis; the parameters are also set. For the positive mode the parameters were peak intensity >5000 and retention time between 1.5 and 20 minutes. The parameters of the negative mode were peak intensity >6000 and retention time between 1.5 and 20 minutes.
5. Review deconvolution
6. Identify compounds. - In this step the user chooses the libraries that are going to be used to look for identifications; the user can choose as many libraries as preferred and set the parameters for each one of them. In out analysis we used three libraries

ChemSpider and Elemental Composition (90%). The parameters for each one of them are shown below:

- ChemSpider

  Precursor tolerance: 5 ppm

  Data sources: KEGG, NIST, NIST Spectra, NIST Chemistry WebBook Spectra, PubChem

  Theoretical fragmentation: off

  Isotope similarity filter: 95%

  Elemental composition filter: C (0-100), H (0-150), O (0-30), N (0-10), P (0-2), S (0-2)

- Elemental composition

  Precursor tolerance: 5 ppm

  Isotope similarity 90.00%

  Elements: C (0-100), H (0-100), O (0-20), N (0-20), P (0-2), S (0-2)

7. Review compounds.- Here is possible to see the relative abundance of the compounds and how they change between samples. It is also possible to create a tag for all the compound found in the experiment designed or to only chose certain compounds that are of interest
8. Compound statistics.- In this section a principal components analysis (PCA) of all the compounds is shown excluding those that have been filtered out. It is important to be careful with the filters in order to have the best PCA for the data.

A thorough explanation of each step can be found in the Progenesis QI manual (Nonlinear Dynamics, 2015) and Peterson, (2016).

For the analysis of the data from the LC-MS analysis we identified all the compounds using the ChemSpider and Elemental Composition libraries. After the identification, all the not identified compounds were filtered and not used for further analysis. After the identification of the compounds, the design of each experiment/comparison was done. For each experiment a filter of molecules that were present in that design with an Anova p-value ≤ 0.05 was applied. Once all the identified compounds with an Anova p-value ≤ 0.05 were filtered, they were tagged in order to mark them as the compounds found in that specific design. The tag was design specific. It was necessary to refresh the filters between experiment designs in order to get the compounds found in the chosen design. After the tagging of the compounds a principal component analysis was performed with the built-in EZinfo software (Version 2.0.0.0, Umetrics AB). The PCA was done to see overall trends of different samples, and the compounds occurring in the samples. The molecular formula assignment will be explained in the compounds identification section.

6.5.4 PCA

A PCA is a statistical method designed to summarize and represent a multivariate data table in a low dimensional plane or model in other words, it is a method of variation reduction that extracts and plots the systematic variation of the data points into a matrix X graph (Ericksson et al., 2013; Starmer, 2015).

The PCAs are commonly used when the data being analyzed has many variables that could be correlated with one another. Using a PCA

allows the identification of the most important variables that explain most of the variation of the data.

As explained in Ericksson et al. (2013), after the PCA is applied, a new set of variables is produced, these are called principal components (PC). Each one of these components explain the variation of the data hierarchically that is, the PC1 (t[1]) is the axes that explains the most variation, the PC2 (t[2]) is the axes that explains the second most variation, and so on (Starmer, 2015).

The projection of these two different components is called a "plane". The plotted observations of the PCA enable the visualization of the dataset structure. The data points plotted in a plane are called "scores" and they represent a map of the samples that shows the grouping of samples or data points that are related to each other. On the other hand, a "loadings plot" shows the variables (loadings) that are affecting the grouping of these different samples. The loadings explain the correlation magnitude (degree of correlation) and manner (positive or negative correlation) of the different variables and thus, the loadings explain how the different variables are interacting in order to produce the scores (Ericksson et al., 2013). When comparing the loadings and the scores plots, it is possible to see what variables are influencing the grouping of the different scores.

6.5.5 Compounds identification

After the identification of compounds by ChemSpider and Elemental Composition, a formula assignation was done. The assignation of a molecular formula to each compound was done taking into account the score, mass error (ppm) and isotopic similarity. All the proposed

formulas containing isotopes or a negative or positive charge were deleted from the compounds list.

The compound formula was assigned based on the greater the score and isotope similarity and the lesser the mass error. The formula assignment was based on the highest probability of the compound being that of the proposed formula. Since no standards were used we were not capable of identifying compounds with 100% accuracy however, the identified formulas are a good approximation.

7 Results

It was possible to see an effect of the long-term low pH conditions on the POC and DOC. The DOC characterized presented differences between pre and post low pH samples as well as over time. The bacterial activity regarding the degradation and uptake of POC and DOC was also affected; it was possible to see a difference in the DOC/C from the bacterial decomposition after the long-term low pH exposure.

7.1 Control experiment (pH 7.7)

In this experiment the natural environmental conditions found in the Baltic Sea (B3 field) were simulated. The chemical and physical parameters of the water inside the TiTank are shown in Fig. 7.1. The temperature, pH, DO and salinity remained quite stable with an average of 9.9 °C, pH of 7.71, 94.4% DO, and salinity 7.2. The Redox potential presented fluctuations but it remained within the oxidizing values. No reducing conditions were reached, as there was an oxic environment inside the TiTank.

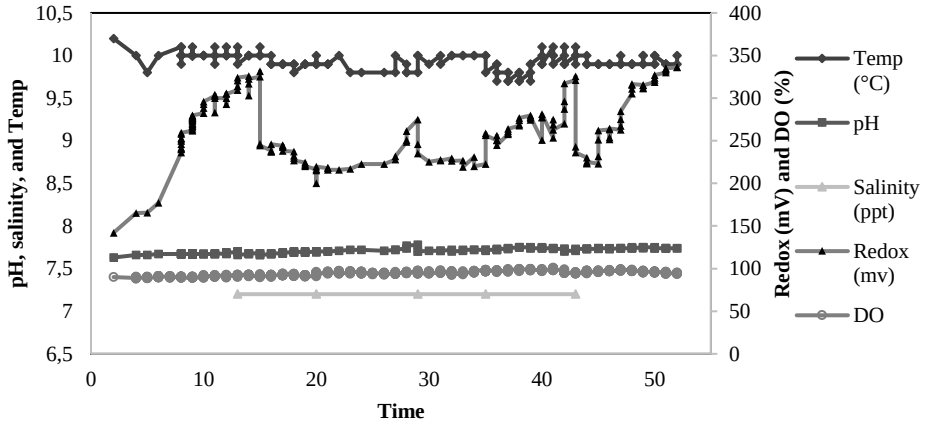

Fig. 7.1 Chemical and physical parameters of the TiTank control Temp: temperature, DO: dissolved oxygen.

7.2 CO_2 seepage experiment (pH: 7.0)

The pH 7 experiment recreated the environmental conditions that would occur in case of CO_2 seepage from the B3 field and the consequent decrease of pH were studied. The chemical and physical parameters of the water inside the TiTank during the pH 7 experiment are shown in Fig. 7.2. The addition of CO_2 into the tank started in day 11 and 12 (marked with a red dotted line). The temperature, DO, and salinity remained stable throughout the experiment with an average of 10.0 °C, 96.7% for the DO, and 6.8 salinity. The redox potential decreased sharply on day 38 however, as there was not a drop in DO, the Redox potential drop could have been caused by some bacterial accumulation around the sensor or some malfunction of the sensor. After the decrease in day 38 the values remained stable again until the end of the experiment. The acclimatization period pH values were stable at 7.7. In the experimental period, CO_2 was added into the TiTank in order to reach a pH= 7, the pH stabilized on day 13. The average pCO_2 was 5030 ± 680 µatm.

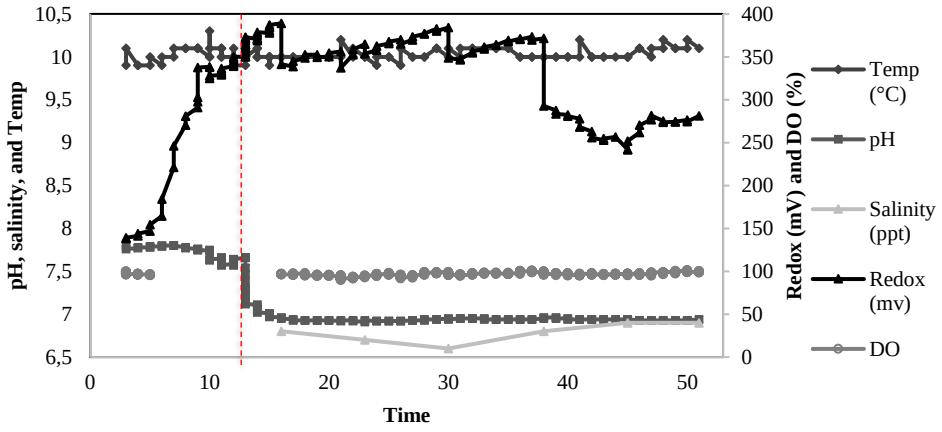

Fig. 7.2 Chemical and physical parameters of the TiTank pH 7
Temp: temperature, DO: dissolved oxygen.

7.3 pCO_2 and DIC parameters

The values of the pCO_2, the different DIC species (HCO_3^-, CO_2 and CO_3^{2-}), calcite and aragonite are shown in Table 7.1. The values show that under the environmental conditions simulated in the TiTank (t= 10°C, S= 7 and pressure= 9 bars) when there is an increase in pCO_2, the molality of HCO_3^-, CO_3^{2-} decreases as well as the Ω of aragonite and calcite.

Table 7.1 pCO_2 and inorganic carbon parameters during the pH 7 experiment
***p*CO₂ average concentration of the control and the pH 7 experiment, dissolved inorganic carbon values of bicarbonate (HCO_3^-), carbonate (CO_3^{2-}), and carbon dioxide (CO_2). Saturation (Ω) of calcite (Cal) and aragonite (Ara).**

	pCO_2 (µatm)	HCO_3^- (µmol/kgSW)	CO_3^{2-} (µmol/kgSW)	CO_2 (µmol/kgSW)	Ω Cal	Ω Ara
			Mean			
Control	1080 ± 50	1952 ± 94	27 ± 2	56 ± 3	0.7 ± 0.1	0.41 ± 0.03
pH 7	5030 ± 680	1806 ± 41	5 ± 1	258 ± 35	0.14 ± 0.02	0.08 ± 0.01

The values of the pH 7 experiment are given after the addition of CO_2 in the system

7.4 DOC

7.4.1 DOC comparison between the control and the pH 7 experiment

Fig. 7.3 shows the comparison between the control and pH 7 outflows. The DOC concentration (mg C/L) from the control experiment showed a stable trend unlike the DOC of the pH 7 experiment. The pH 7 experiment DOC values increased after the addition of CO_2 (red dotted line) and decreased towards the end of the experiment. The Δ value between the inflows and outflows of the control was -0.04 and for the pH 7 experiment was 0.2. The comparison between the inflow and outflow of the control, and pH 7 experiment are shown in appendix Fig. 11.1 and Fig. 11.2.

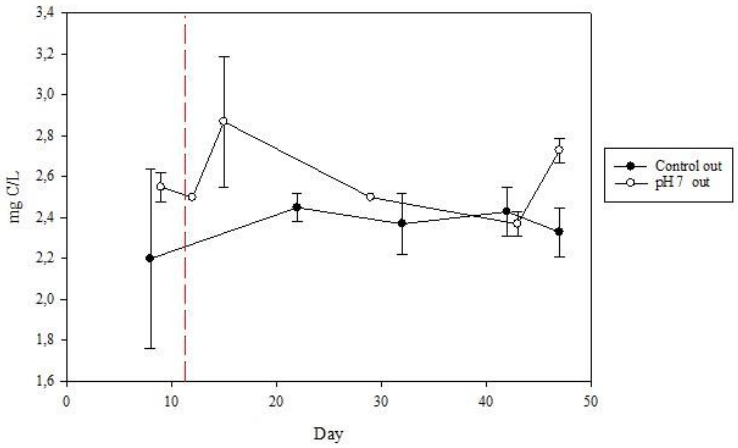

Fig. 7.3 DOC values comparison

7.5 POC

7.5.1 POC comparison between the control and the pH 7 experiment

The POC concentration (µg C/mL) of the control experiment outflow remained stable throughout the experiment. Contrastingly, the POC values of the pH 7 experiment outflow increased after the addition of CO_2 (red dotted line) and then showed an overall decrease (Fig. 7.4). The Δ value between the inflow and outflow of the control was 0.01 and for the pH 7 experiment was 0.002. The comparison between the inflows and outflows of the control and pH 7 experiment are shown in the appendix Fig. 11.3 and Fig. 11.4.

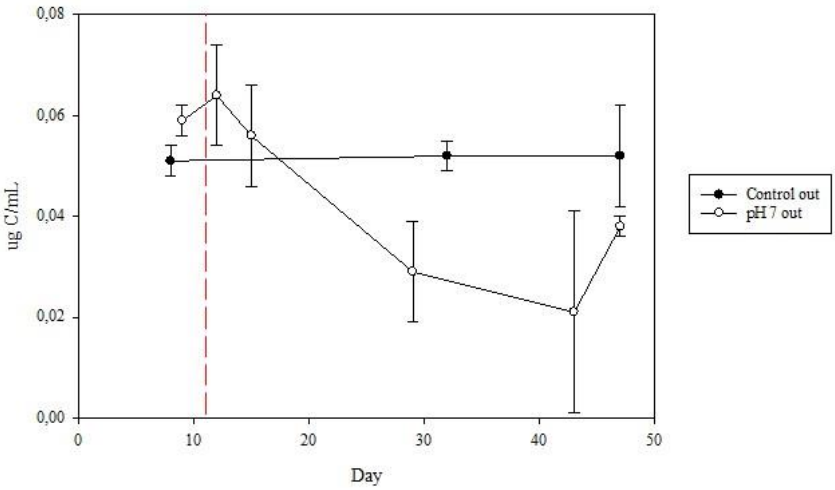

Fig. 7.4 POC values comparison

7.6 DOC/C

All the results from the DOC/C of the control and pH 7 experiment results will be shown from both positive and negative mode analysis. The presentation of the results with a PCA comparison will be presented first, and later the comparison of the molecules found with an Anova ≤ 0.05 in each experimental design.

7.6.1 Comparison of the control, and the pH 7 experiment acclimatization period

The PCA of the comparison between all the outflows of the control experiment and the pH 7 experiment acclimatization is shown in Fig. 7.5. In the positive mode scores plot (Fig. 7.5b), the scores belonging to the acclimatization period of the control experiment (day 8) are different from those of the middle (day 32) and end (day 47) of the control

experiment. The scores of day 32 and day 47 are clustered and thus are not different from each other.

The pH 7 experiment acclimatization period was maintained at a pH= 7.7 and all the conditions in the TiTank were equal to those of the control. Nevertheless, the scores from the pH 7 experiment acclimatization period (day 9) are clustered together and are different from all the scores of the control experiment acclimatization and experimental period. The loadings plot (Fig. 7.5a) shows the compounds found and their distribution in the samples.

A similar difference is seen in the negative mode analysis Fig. 7.5d where the scores from the outflows of the acclimatization period of the pH 7 experiment (day 9) are different from those of the control experiment (day 8, 32 and 47). In the control experiment negative mode, the scores from the acclimatization period (day 8) are different from the experimental period samples scores (day 32 and 47). There was a higher amount of compounds (loadings) found in the negative mode; their distribution in the samples is shown in Fig. 7.5c.

The DOC/C from the acclimatization period (pH=7.7) of the pH 7 experiment was different from the DOC/C from the control experiment samples (pH=7.7). Due to the differences in DOC/C between the control experiment samples and the pH 7 experiment acclimatization period samples it was decided to use the pH 7 experiment acclimatization period samples as the control for the pH 7 experiment.

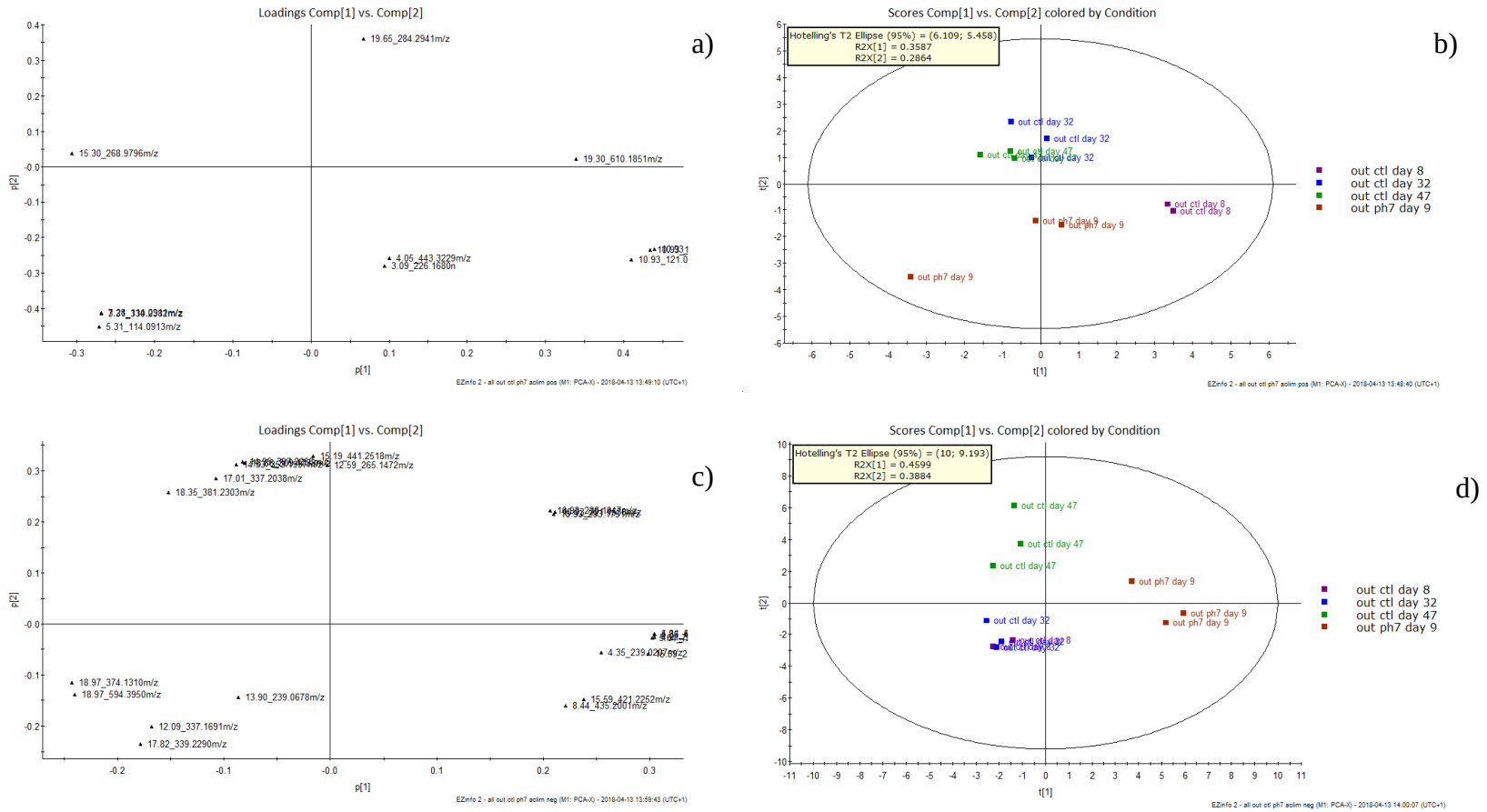

Fig. 7.5 Comparison between all the outflows of the control experiment and the outflow of the pH 7 experiment acclimatization period (10 days) Positive mode. a) loadings and b) scores, and negative mode c) loadings and d) scores.

7.6.2 DOC/C pH 7 experiment

pH 7 experiment inflows and outflows DOC/C

In this section a comparison between all the inflows and outflows of the pH 7 experiment was performed in order to see any differences between the acclimatization and the experimental period. The PCA analysis in positive mode (Fig. 7.6a and b) and negative mode (Fig. 7.6c and d) are shown bellow. The scores (Fig. 7.6b) from the positive mode analysis show that the samples from the acclimatization period are clustered together whereas the samples of the experimental period shift from quadrant I and IV towards quadrant III. The loadings (Fig. 7.6a) show three different clusters and they are related to the change in the molecular composition of the samples over time.

The scores plot from the negative mode (Fig. 7.6d) shows that the outflow acclimatization samples and the experimental samples are clustered together in the middle of the graph meaning that they are not different from one another; the only samples that are outside this cluster are those of day 47. The samples trend is not as clear in the negative mode as it is in the positive mode plot (Fig. 7.6b). Regarding the loadings (Fig. 7.6c), the compounds shift went from right to left in an anticlockwise direction. The right to left shift over time in both graphs is explained by changes in the water quality. In the positive mode t[1] accounts for 36% of the variation, and in the negative mode for 43% and thus there is a stronger effect of the water quality in the negative mode compounds. On the other hand, the difference between the inflow and outflow in the positive mode scores plot t[2] (22%) is explained by the effect of the addition of CO_2 into the TiTank and thus the effect of the low pH conditions is affecting the positive mode compounds more than the negative mode compounds.

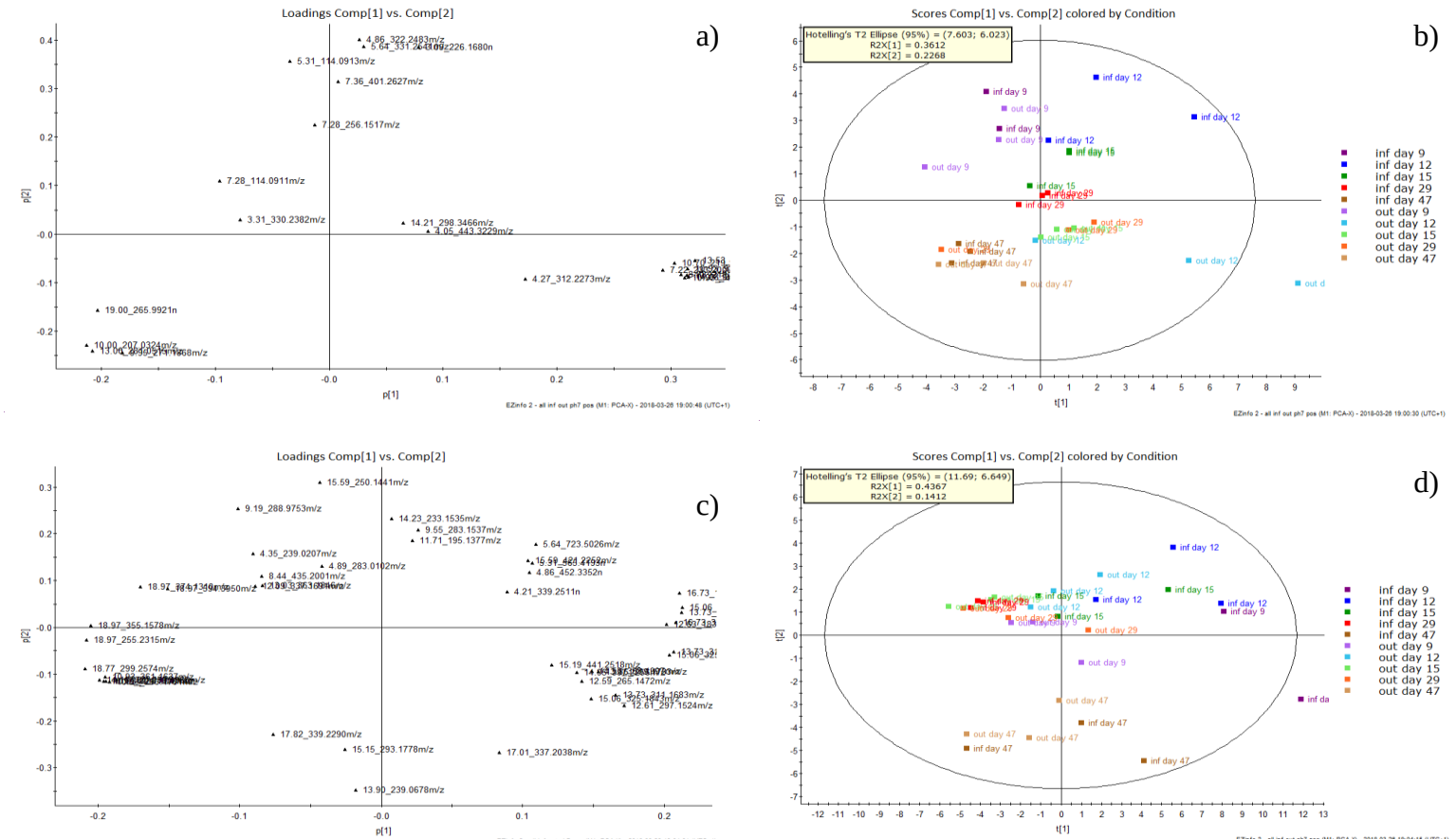

Fig. 7.6 Comparison between all the inflows and outflows of the pH 7 experiment Positive mode a) loadings and b) scores and negative mode c) loadings and d) scores

7.6.3 DOC/C: identifications

The amount of identified molecules per sampling day with an Anova p-value ≤ 0.05 for the positive and negative mode is shown in Fig. 7.7. After the addition of CO_2 (red dotted line) into the tank there was a clear shift in the amount of molecules that were identified.

The lists of identified compounds of the pH 7 experiment in the positive and negative mode are shown in the appendix section 2 Table 11.1 and Table 11.2. The compounds identified had a MW of < 1000 Da; the compounds will be separated in three categories: small (0-300 Da), medium (301 to 600 Da) and large (601-1000 Da).

The amount of identified compounds in the positive mode is 39 and in the negative mode 35. In both modes, the majority of compounds belonged to the inflow, 24 in the positive and 21 in the negative. In the positive mode there is a shift in the compounds from medium-big to small compounds throughout the experiment. In the negative mode the shift seems to be from small to medium sized compounds.

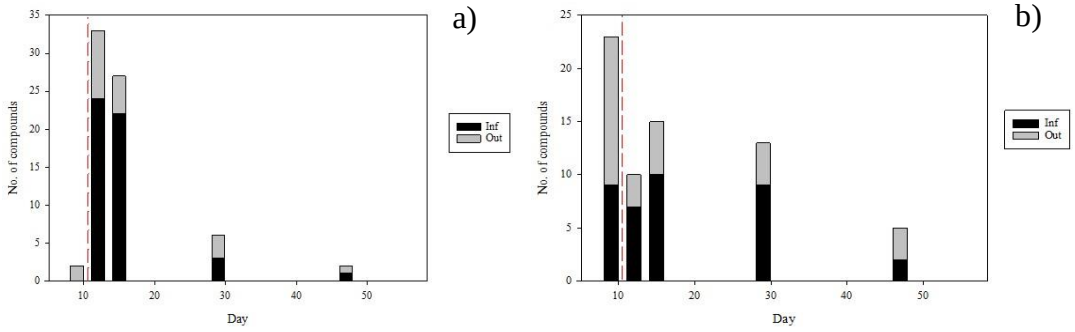

Fig. 7.7 Amount of identified compounds overtime during the pH 7 experiment
a) Positive mode, b) negative mode

7.7 BD

For the bacterial decomposition experiment the results of the DOC and POC from the outflows will be shown along with those of the pre decomposition this, in order to show how the values changed from the initial condition. A thorough explanation of this experiment is found under the methods section.

7.7.1 DOC BD

DOC comparison between pre and post BD from the control and the pH 7 experiment

The comparison between the DOC mean concentration (mg C/L) from the pre and post bacterial decomposition of the control and the pH 7 is presented in Fig. 7.8. In the acclimatization period of both cases, the post decomposition concentration is greater than that of the pre decomposition samples. However, in the middle of the pH 7 experiment, after the addition of CO_2 (red dotted line), the DOC values are greater in the pre decomposition samples than in the post decomposition samples.

The Δ values of the control experiment pre versus post decomposition samples had an average value for the inflow of 0.1 and the outflow of 0.2. The Δ values of the pH 7 experiment had a value of 0.53 for the inflow samples and 0.13 for the outflow samples. The inflow pre and post decomposition for both the control, and pH 7 experiments are shown in the appendix Fig. 11.5 and Appendix Fig. 11.6.

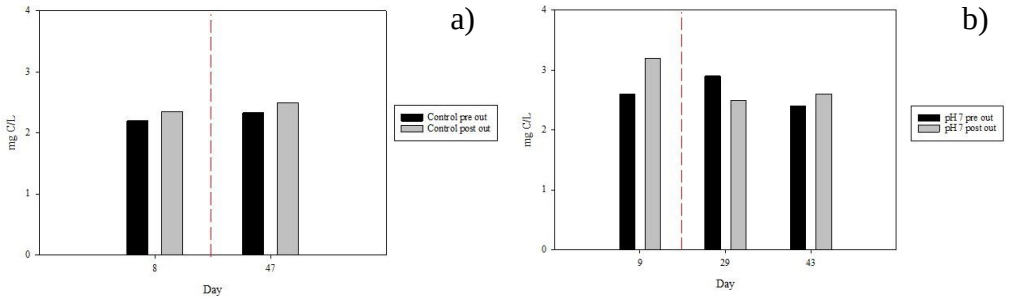

Fig. 7.8 Comparison of the pre and post decomposition DOC values a) Control, and b) pH 7 experiment.

7.7.2 POC BD

POC comparison between pre and post BD from the control and the pH 7 experiment

Fig. 7.9a is showing the pre and post decomposition POC concentration (µg C/mL) of the control experiment and Fig. 7.9b is showing the pre and post decomposition POC values of the pH 7 experiment, the addition of CO_2 is marked with the red dotted line. In both cases the POC experiences a decrease after the bacterial decomposition. Regarding the pH 7 experiment the amount of POC available in the initial condition decreased over time. The Δ values of the control experiment pre versus post decomposition samples had an average value for the inflow of -0.04 and the outflow of -0.03. The Δ values of the pH 7 experiment had a value of -0.02 for the inflow samples and -0.01 for the outflow samples. The inflows of the control and pH 7 experiments are shown in the appendix Fig. 11.7 and Fig. 11.8.

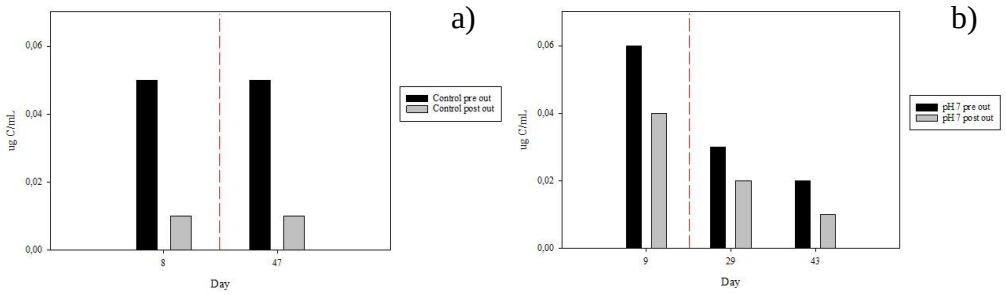

Fig. 7.9 Comparison of the post decomposition POC concentration a) Control, and b) pH 7 experiment.

7.7.3 DOC/C BD

Post BD inflows and outflows comparison

The post BD inflow and outflow of the control and pH 7 experiment in the positive mode are shown in Fig. 7.10. In both experiments and modes the inflow and outflow samples of the acclimatization period were different. In all cases, the acclimatization samples were different from the experimental period samples. This difference was greater that the difference between the experimental period samples. The negative mode comparison is shown in appendix Fig. 11.9.

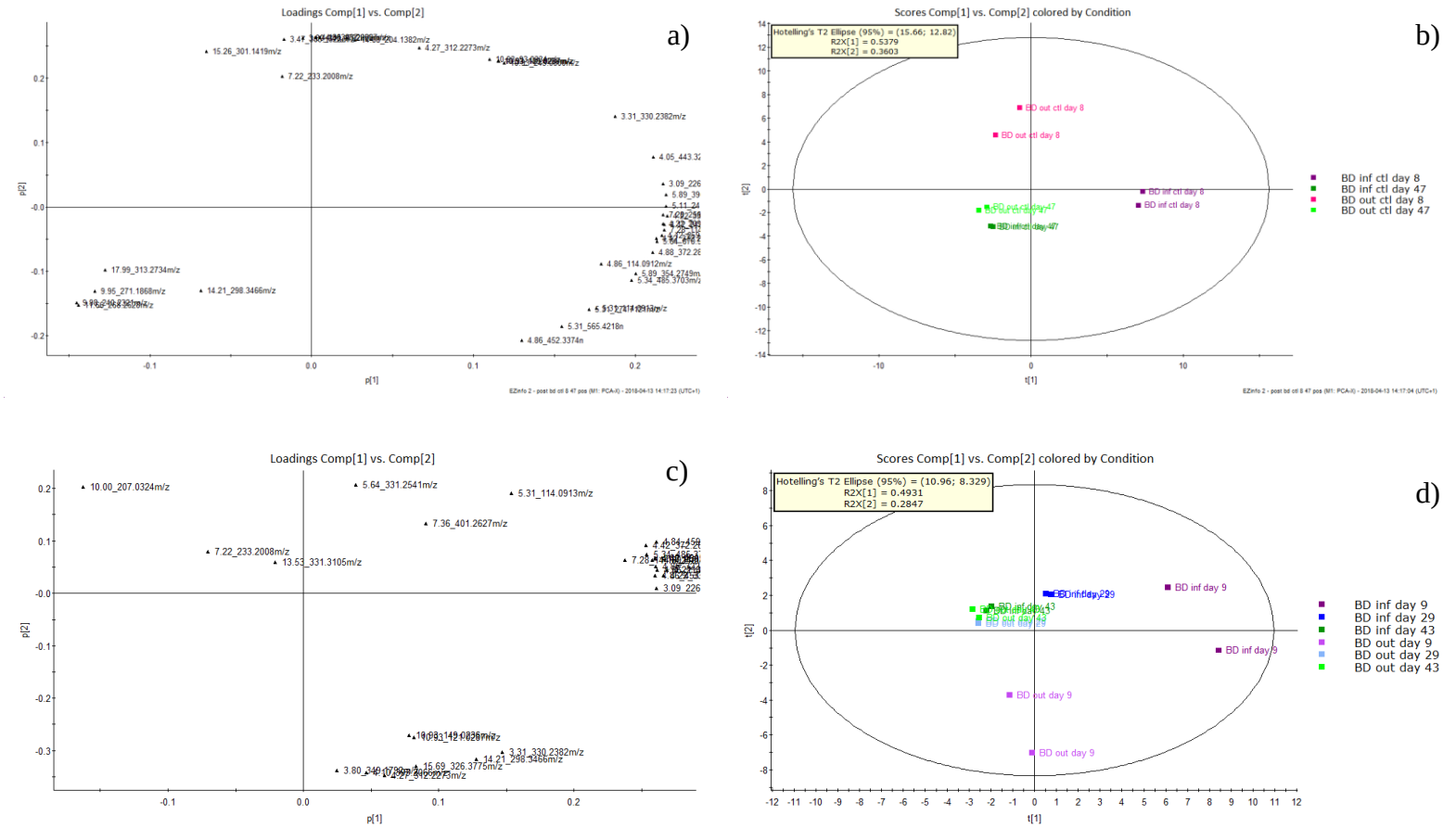

Fig. 7.10 Inflow and outflows after bacterial decomposition positive mode Control a) loadings and b) scores and pH 7 experiment c) loadings and d) scores

DOC/C BD: identifications

Pre and post BD day nine and 29 pH 7 experiment

The comparison between the pre and post decomposition samples was done with the samples from the pH 7 acclimatization day 9 and from the experimental period day 29. The compounds of the pre and post decomposition inflow and outflow for day 9 and 29 in both positive and negative mode are shown in the appendix section 2 Table 11.3 and Table 11.4.

In the positive mode (appendix Table 11.3) the highest amount of identified compounds is found in the pre decomposition inflow samples of day 29. There were 42 identified compounds. Day 9 showed 25 compounds in total and 11 were found in the post BD samples. Two of the compounds were shared between the inflow and outflow post BD samples. The samples from day 29, showed 35 compounds; none of these compounds were shared between post BD samples.

In the negative mode, 36 compounds were identified in total. Of these compounds, 30 were detected in the samples from day 9 and two of the compounds were shared between post BD samples of the inflow and outflow. The highest amount of identified compounds was found in the inflow pre decomposition sample of day 29. The samples of day 29 showed 23 compounds. None of these compounds were shared between post BD samples from the inflow and outflow.

Comparison between post BD samples of the pH 7 experiment

The comparison between all the post decomposition samples of the pH 7 was made in order to see how the compounds changed over time. The tables with

all the identified compounds are found in the appendix Table 11.5 and Table 11.6.

In the positive mode (appendix Table 11.5), the samples with the highest amount of identified compounds were the outflows. The post decomposition inflow and outflow samples of day 9 share three compounds whereas those of day 29 share one compound. All the post decomposition outflows (day 9, 29 and 43) are different and do not have any compounds in common. There were no compounds shared within inflows or outflows.

In the negative mode (appendix Table 11.6), three compounds were shared between the post decomposition inflow and outflow samples for day 9 and 29. No compounds were similar between days 9, 29, and 43.

8 Discussion

One of the keys to understanding the effects of OA and the changes in the marine OC is to acknowledge that the marine inorganic and organic carbon are closely related and one affects the other. The process of OA affects the solubility pump first and later, the BCP and MCP. As a consequence of the changes produced by low pH conditions, the ocean capacity to store carbon and the marine life are compromised (Feely 2004; Doney et al.,2009; Jiao et al.,2014).

The main difference between the pH changes induced by the localized seepage of CO_2 from CCS sites and those of OA caused by atmospheric CO_2 absorption is that the affected organisms can migrate away from a CO_2-seepage site, whereas in the event of OA due to atmospheric CO_2 intake their only option is to adapt or die (Blackford et al., 2009).

8.1 Experimental design

Recent studies have focused on studying the effects of OA in superficial waters (1atm) (Riebesell et al., 2013; Engel et al., 2014; MacGilchrist et al., 2014; Zark et al., 2015; James et al., 2017); others have addressed the potential effects of CO_2 seepage from a CCS site (Yamada et al., 2013; Molari et al., 2018). These studies have provided extensive information about the effects of OA and the associated risks of seepage from a CCS site however; they have not addressed the long-term effect of low pH under high-pressure conditions.

The novelty of the CO_2Marine experiment and the TiTank system was that by manipulating the physical parameters and using sediments and animals from the Baltic Sea, it recreated the natural conditions found in the prospected CCS site B3 in the Baltic Sea. The TiTank experiment was designed to show the effects that a low pH event would have on the

sediments, two benthic species, marine organic chemistry, and bacterial heterotrophic activity. The system was under nine bars of pressure, a continuous flow of seawater, and under long-term low pH stress. In addition, the system was in complete darkness and thus no photosynthetic activity was possible. This experiment was unprecedented in terms of the realistic recreation of the natural environmental conditions of the proposed CCS site.

As mentioned before in the materials and methods section, the seawater used in the experiment was artificially adjusted to recreate the S, T, TA, and pH of the Baltic Sea seawater. The experiment was performed in Trondheim, Norway and it had a continuous flow of seawater throughout the experiment, thus making it logistically impossible to bring water from the Baltic Sea. One of the consequences of using water from the Trondheim´s fjord in the experiment was that the bacterial and algal communities were not native to the Baltic Sea. The difference in the plankton community could affect the types of DOC released from bacterial degradation and the different EOC from the primary producers, thus altering the DOC/C and composition, however this has not been proven beyond doubt (Søndergaard and Middelboe, 1995).

The aim of this study was to investigate the possible effects that long-term, high-pressure, low pH conditions would have on the POC, DOC, DOC/C and on the BD of DOC. The results produced in this thesis are a valuable initial approach to the study of the effects of high-pressure long-term low pH stress on the different OC species and the bacterial community. The findings of this thesis serve to provide information about the changes experienced by the LDOC and RDOC in the seawater and the effect that a long-term high-pressure low pH stress had on the bacterial community capacity to degrade OC and transform it into RDOC.

Regarding the experiment execution, the sampling plan was satisfactory as it allowed for the study of the acclimatization period of the tank, the first rapid changes after the addition of the CO_2, and the stabilization period towards the middle and end of the experiment. Moreover, previous studies related to DOC/C have neglected the study of the positive mode fractions focusing on the characterization of the negative mode fraction (Koch et al., 2008; Zark et al., 2015). Contrastingly, in this thesis, the DOC/C approach was more comprehensive as the DOC/C analysis considered the compounds found in both positive and negative mode.

8.2 Physical and chemical parameters of the TiTank

8.2.1 Control experiment

The peaks observed on the redox potential appear to have been caused by disturbances associated to the sediment sampling from the carrousel. The peaks of day 15, 43, and at the end of the experiment correlate to the sediment sampling days. The jump from day 27 to 29 appears to be related to the swap of the redox sensor, which was changed in day 27, there was no sediment sampling from day 27 to 29.

8.2.2 pH 7 experiment

The T, DO, and S remained constant during the pH 7 experiment. The only difference between the control and the pH 7 experiments relies on the difference in pH between the treatments. It is important to point this out because the aim of the experiment was to focus on the changes associated to low pH stress, and not the effect of multi-stressors.

8.3 Water samples

8.3.1 DOC

The experiments were performed during the Fall-Winter period from November 2016 to March 2017. During this period, the destratification of the water column in the fjord occurs making the water chemistry more homogeneous (Børsheim et al., 1999). The natural variations of the inflow water from the fjord did not affect the performance of the TiTank or the outflow values; the TiTank had a stabilizing effect on the DOC concentration detected in the outflow. The negative Δ of the control experiment shows that there was a slightly higher amount of DOC in the inflow than in the outflow, and thus that the DOC from the inflow was being consumed inside the TiTank.

On the other hand, the DOC from the pH 7 experiment outflow samples shows fluctuations. A short term experiment has reported mobilization of DOC between sediments and seawater under short-term low pH stress (Martín-Torre et al., 2013). It is possible that the DOC fluctuations seen in the pH 7 experiment are related to the initial mobilization of DOC from water to sediments. However, after long-term exposure to low pH conditions, an increase in the concentration of DOC in the water was detected, followed by a steady decrease towards the middle and end of the experiment. It is necessary to further study the mobilization of DOC between sediments and seawater under long-term pH stress.

Even though, the concentration of DOC in the outflow decreased over time it was higher than the concentration of DOC in the inflow. This is reflected in the positive Δ in the pH 7 experiment. The DOC decrease in the outflow could be related to an enhanced enzymatic activity of the bacteria (Piontek et al., 2013) and an enhanced respiration (James et al., 2017). The results also show an increase in the concentration of DOC in the water at the

end of the experiment. It is necessary to further study the long-term effect of low pH on the DOC compounds chemistry, as well as on the extracellular enzymatic activity and adaptive capacity of the bacteria, this in order to determine the changes in the degradation and production of the different species of DOC.

8.3.2 POC

During the control experiment the POC values of the inflow varied over time. However this did not affect the values of POC of the outflow, which remained stable during the experiment. Due to the stabilized values seen in the outflow DOC and POC, in relation to the inflow of the control experiment, we concluded that even when there were variations on the inflowing water, the conditions inside the TiTank were not affected by the inflow fluctuations.

The positive Δ of both the control and pH 7 experiments highlight how there was a higher concentration of POC in the outflows than in the inflows. Nevertheless, the control experiment $\Delta = 0.01$ is an order of magnitude larger than the pH 7 experiment $\Delta = 0.002$. This means that the control outflow had a greater amount of POC with respect to the inflow than the pH 7 experiment outflow to the inflow.

The TiTank had three sources of POC in both the control and the pH 7 experiment; the POC came from the water, the added algae, and the sediment. The POC from the inflow accounts for two of the three possible sources of POC into the tank, and thus whatever increases in the POC of the outflow compared to the inflow were related to a process happening inside the tank.

The outflow POC values of the pH 7 experiment showed an overall decrease, reaching values lower than those of the control experiment. This decrease indicates that the variations in the POC concentration were due to

the effect of low pH in the system, and were not caused by variations in the different POC sources. We propose that the decrease over time in the POC concentration of the pH 7 experiment outflow, as well as the lower Δ when compared to the control was caused by the effect of the high pCO_2. The low pH enhanced the hydrolysis and breakdown of the POC mediated by an increased bacterial enzymatic activity (Grossart et al., 2006; Piontek et al., 2010) and increased bacterial respiration inside the TiTank (James et al., 2017). These two processes consumed the POC inside the TiTank causing a decrease over time and shortening the Δ.

8.3.3 DOC/C

Comparison of the control, and the pH 7 experiment acclimatization period

Regarding the control experiment samples, the PCA analysis shows that there is a difference between the acclimatization period samples and the experimental period samples of the control experiment in the positive and negative mode. This difference shows that at the beginning of the experiment in the acclimatization period (day eight), the DOC/C was different from the DOC/C of the middle and end of the control experiment (day 32 and 47). In the experimental period of the control (day 32 and 47) the DOC composition became more similar; this happened in both the positive and negative mode. It is possible that the difference in the acclimatization period was due to the initial interaction between the water and sediments; and to the exchange of DOC between them. Nevertheless, over a longer period of time this exchange of DOC inside the TiTank stopped or was stabilized and the difference in DOC was not as great as in the beginning. These results along with those obtained from the DOC and POC, support the assumption that the conditions

inside the TiTank allowed the stabilization of OC found in the outflow samples.

The positive and negative mode PCAs showed a difference between the acclimatization periods of the control and the pH 7 experiment. This indicates that the acclimatization periods did not have the same starting point with regard to the DOC/C composition. Due to this difference, the acclimatization period samples of the pH 7 experiment would serve as the control samples for all the samples obtained from the pH 7 experiment experimental period.

pH 7 experiment inflows and outflows DOC/C

In the positive mode PCA, the acclimatization period samples (day nine) were different from all the other samples of the experimental period. The experimental period samples shift from right to left, indicating that there was a change in the quality of the inflowing water over time. This can be concluded because the samples from the inflow and outflow shifted in parallel towards the left of the PCA. This effect accounts for 36% of the variation but it did not overshadow the effect of the low pH treatment. The low pH effect was seen in the difference between the inflow and outflow samples for each sampling day and helps to explain 22% of the variation.

Regarding the negative mode, the compounds showed no clear time trend and there was not a clear difference between the acclimatization and experimental period compounds. We suggest that the charge of the negative compounds was affected by the increased amount of protons in the water, and thus the compounds became protonated (Roggatz et al., 2016).The protonation of the negative compounds caused them to become apparent in the positive mode PCA, thus showing that there was an effect of the low pH conditions on the compounds found in the positive mode but not in the negatively charged compounds.

8.3.4 DOC/C: identifications

All the compounds identified and characterized are LMW compounds of <1000 Da. In this thesis the differentiation between the compounds will be done as follows: small (0-300 Da), medium (301 to 600 Da) and large (601-1000 Da), this categorization is merely used for distinguishing the compounds.

In the pH 7 experiments, the positive mode had a higher incidence of compounds. As previously indicated, this may be due to a conversion of compounds that shifted from being negatively charged to positively charged. In both positive and negative mode, the compounds changed from big and medium compounds to smaller sized compounds. It has been previously reported that under acidified conditions, the organic compounds undergo enhanced hydrolysis (Doney et al., 2009; Piontek et al., 2013; James et al., 2017). The change in the MW of the compounds was in accordance with what has been previously reported by Ogawa and Tanoue, (2003) where compounds of a HMW were more labile than LMW compounds.

Some compounds appeared repeatedly in several inflows or outflows regardless of the sampling day. The compounds that appeared in 3 or more sampling days will be called “persistent”. In the positive mode, the inflow of the experimental period presented two persistent compounds with MW of 114.0912 and 227.1753 Da. The outflow presented just one persistent compound with a MW of 330.2382 Da. This compound was found in all the outflows, with the exception of the last sampling day (day 47).

In the negative mode, two big compounds with MW of 610.4183 and 723.5026 Da were persistent in all the inflows and one medium-sized compound (MW 497.3343 Da) was found in three of four experimental period days. In the outflows, all of the persistent compounds were medium sized; one was present in all of the outflows (MW 337.1691 Da) and another

compound (435.2001 Da) appeared three times, one in the outflow of the acclimatization period and in two of the experimental period days.

The persistent compounds in the inflow samples are important because they appear in the water regardless of the water quality. The compounds persisting in the outflow appear regardless of the low pH in the water, thus the processes producing these compounds were not affected by the low pH conditions.

8.4 BD

8.4.1 DOC BD

The DOC concentration values of the control outflow showed an increase after the BD; the positive Δ between the BD inflows and outflows showed that there was an enhanced production of DOC in the outflow samples. The extra DOC in the samples is RDOC. The increase in the DOC concentration may be explained by the degradation of POC by the heterotrophic bacteria (Jiao et al., 2010)

In the pH 7 experiment, there was an increase in the concentration, and thus the production of DOC in the outflow post BD samples of the acclimatization (day nine) and day 43. The lower concentration of DOC in the samples of day 29 is likely related to the contamination of one of the triplicates of the pre decomposition sample, and not to the bacterial activity. Nevertheless, the negative Δ between the BD inflow and outflow shows a decreased concentration of DOC in the outflow. The low pH exposure affected the bacterial degradation and transformation of DOC resulting in a lower production of RDOC species after long-term low pH stress.

8.4.2 POC BD

In both the control and pH 7 experiment, the rate of consumption in the acclimatization period outflow was higher than that of the experimental

period. The amount of POC available for BD decreased over time in the pH 7 experiment; the decrease may have been caused by processes that happened inside the TiTank.

The negative Δ of the pre versus post BD inflows and outflows of both experiments show that there was a higher amount of POC in the pre BD samples, and thus that the POC was degraded by the bacterial activity. This is in accordance with the positive Δ found in the DOC after the BD, since after the bacterial degradation the POC is transformed into DOC (Jiao et al., 2010; Piontek et al., 2013). However, when comparing the inflows versus outflows, the control experiment Δ is 0.002, and 0.01 for the pH 7 experiment. The positive values show that there was an overall higher concentration of POC in the outflow samples; these results are in accordance with what we found for the POC in the water samples.

The Δ of the pH 7 experiment is an order of magnitude larger than that of the control. This difference may be the result of enhanced degradation of the POC, caused by the effect that the low pH had on the enzymes produced by the bacteria (Piontek et al., 2013; James et al., 2017). In our experiment, we did not see the aggregation of DOC into POC or the eventual formation of TEP´s, this is different from what Yamada et al. (2013) and Engel et al. (2004, 2014) have reported before.

8.4.3 DOC/C BD

Post BD inflow and outflows comparison

In the control experiment samples, the PCA in positive and negative mode showed a difference in the DOC characterized between the pre and the post decomposition samples. The difference between the pre and post acclimatization period samples may have been caused by the flushing of the bacteria that were in the sediments into the water. After the initial flushing of

the sediment bacteria, the bacterial community inside the TiTank was homogeneous between the inflow and the outflow. This may have been the reason behind the difference in the beginning of the experiment (in day eight) and the convergence on day 47.

In the pH 7 experiment, it appears that a similar flushing of bacteria occurred, accounting for the difference seen in the positive mode PCA between the acclimatization and the experimental period samples. Regarding the similarity between the samples from day 29 and 43, this would suggest that the bacterial activity was resilient to the low pH stress and once the stress was gone they went back to their normal state. Indeed, a similar response has been previously reported by Borrero-Santiago et al. (2017). This explanation is feasible since the bottles used for the post decomposition experiment were not exposed to low pH stress for a time span of five days. On the other hand, in the pH 7 experiment negative mode PCA, the samples from the acclimatization and experimental period presented greater differences than those of the positive mode. It would appear that the bacteria are decomposing the positive and the negative molecules in a different manner, accounting for the difference seen in the PCA.

8.4.4 DOC/C BD: identifications

Pre and post BD day nine and 29 pH 7 experiment

In the BD experiment of the pH 7 experiment samples, no compounds were found simultaneously in the pre and post BD samples. In other words, none of the compounds found withstood the decomposition. All the compounds found in the post BD samples were newly generated. There were no similar compounds between the inflows or outflows of the pre and post decomposition samples. No post decomposition compounds were similar between the acclimatization and experimental period samples. In the

negative mode, two compounds were shared between the post decomposition inflow and outflow samples from day nine. Within the samples from day 29, no compounds were found in the post bacterial decomposition inflow and outflow.

The compounds shared between post BD samples are of special interest because they are transformed in a similar way regardless of the water being from the inflow or from the outflow. This demonstrates that the water quality did not affect the bacterial decomposition.

When comparing pre and post BD samples, for each inflow and outflow, it was possible to see an apparent shift towards smaller sized compounds. This shift shows the bacterial enzymatic degradation of compounds HMW into LMW compounds. This result is in accordance with what has been previously reported by Piontek et al. (2013) and Jørgensen et al. (2014). Moreover, our findings support the notion of HMW DOC being more reactive than LMW DOC (Amon and Benner, 1996; Ogawa and Tanoue, 2003) and thus LMW DOC being part of the RDOC pool (Ogawa and Tanoue, 2003; Jørgensen et al., 2014).

There were no compounds shared between pre and post BD samples of the inflow or the outflow. Thus means that all the compounds found in the pre BD samples were transformed after the BD or that they were present in the sample but their concentration decreased to levels that reached the LC-MS detection capacity (Brophy and Carlson, 1989; Dittmar et al., 2008).

The compounds found in the post BD samples were produced after bacterial decomposition. Taking into account what has been previously reported about the short lifespan of LDOC (hours to days) (Hansell, 2013) and the time necessary to see the compounds produced after bacterial degradation (within six days) (Jørgensen et al., 2014) we suggest that the compounds that were shared between the post BD samples are potentially

recalcitrant species of DOC because they either withstood degradation or were newly produced and not consumed.

Comparison between post BD samples of the pH 7 experiment

A comparison between all the post bacterial decomposition inflows and outflows was performed. In the positive mode, the inflow and the outflow of the acclimatization period, day nine, were different and only shared three compounds. The difference between the day nine post BD inflow and outflow samples can be attributed to the effect of the TiTank on the water. In the samples of day 29, only one compounds was shared between post BD samples from the inflow and outflow. No compounds were shared between samples for day 43 samples.

In the negative mode, the amount of identified compounds was lower than that of the positive mode. In day nine, three compounds were shared between the post BD samples of the inflow and outflow. Three compounds were also shared between the post BD inflows and outflows of day 29. The compounds that were shared between post BD inflows and outflows are considered to be recalcitrant. These compounds are interesting since they were produced regardless of the low pH stress conditions.

There was an overall lower incidence of compounds in the post BD inflows than in the post BD outflows. This occurred in both the positive and negative mode and may have been caused by an enhanced bacterial activity after the low pH stress that in turn produced more compounds after the BD of the outflows (Jiao et al., 2010; Piontek et al., 2013; James et al., 2017).

Moreover, all the compounds that were identified in this experiment are not LDOC compounds. We can infer this since they withstood bacterial degradation and were found in the samples after five days of decomposition. The compounds found in the post decomposition experiments are considered

to be recalcitrant compounds. The identified compounds have a LMW that ranged from 90 to 730 Da. This finding is in accordance with previous reports that suggest that the RDOC pool is comprised of LMW compounds (Ogawa and Tanoue, 2003).

9 Conclusion

The ocean acidification process caused either by the dissolution of atmospheric CO_2 in the seawater or the seepage of CO_2 from a CCS can affect the chemistry of the organic and inorganic marine carbon, as well as the biology of the marine organisms. The ocean acidification process is currently occurring in the top water column and has not reached yet the deep waters. The increasingly popular utilization of CCS techniques as an alternative to mitigate CO_2 emissions into the atmosphere could change this. In the case of an unrecognized or poorly addressed seepage event from a CCS storage site, the deep water will start to be acidified by CO_2 and thus, the stress in the seawater chemistry will not only occur from the surface but also from the bottom.

Due to the unknown risks associated with a CCS seepage event and the effects of high-pressure long-term low pH on the marine DOC and the marine organisms, it is crucial to develop techniques and experiments that could allow us to understand the potential effects. In this regard, this thesis project as part of the CO_2Marine project showed that under high-pressure, long-term low pH conditions, the DOC, POC and DOC/C of the water samples were affected. After the addition of CO_2, the outflows DOC and POC concentrations had an overall increase with respect to the inflows. The outflows DOC and POC presented a decrease over time under low pH stress. The DOC/C was mainly affected by the water quality but the effect of the low pH was the second most important factor. There was a higher number of positive compounds identified; the effect of the low pH conditions was more conspicuous in such compounds than in the negative compounds. The DOC/C persistent compounds found in the inflow were not affected by the water quality and those of the outflow were not affected by the low pH exposure.

The BD samples of the pH 7 experiment showed an increase in the post BD DOC concentration and a decrease of the POC concentration. In the DOC/C, a higher number of positive compounds were identified than negative compounds. The amount of identified compounds in the pre BD samples was higher than in the post BD samples. The compounds identified after the BD either survived the decomposition or were newly produced by the bacterial activity. The compounds that were found in both post inflow and outflow samples of each day were not affected by the BD or were similarly decomposed.

In other words, the low pH conditions affected all the parameters studied in this experiment. We are confident with the approach taken in this thesis regarding the identification of DOC species as we were able to identify ten compounds that were not affected by the water quality or low pH conditions and 11 compounds that can potentially be part of the RDOC. The results obtained in this project serve as an example of the possible shifts experienced by the marine OC in the case of a seepage event or OA in the deep ocean.

10 Recommendations

The different bacterial communities and algae species may react in a different manner to a low pH stress. Thus, in ideal circumstances, a complete characterization of the bacterial community being used in the experiment would be advisable. It is also important to bear in mind the constraints associated with sediments´ heterogeneity and the potentially different effects of low pH stress on the different sediments.

The stabilization of the system caused fluctuations in the beginning of the control and the pH 7 experiment. It is recommended to have a longer acclimatization period that allows its complete stabilization. The addition of CO_2 should preferably start after no more fluctuations are detected in the different parameters such as S, T, Redox, pH, DOC, and POC. In addition, due to time, equipment, and human resources constraints, the number of samples taken in this study was sufficient but no ideal. As such, we recommend that, in following studies, a bigger sample size is taken in order to perform a more extensive statistical treatment.

Regarding the bacterial decomposition studies under low pH stress, we suggest a characterization of the bacterial community in order to see changes in the bacterial community due to low pH stress. The five days allowed for the BD of the samples was sufficient to see the consumption and production of LDOC and RDOC. However, if the intension is to see the progression in time of the different compounds and change in the ratio of LDOC:RDOC, we would recommend a sampling schedule that covers the whole time span used for the decomposition experiment.

In some cases, the differences in the DOC/C are more noticeable in the LC-MS positive mode than in the negative mode. Future studies should analyze the compounds in both the positive and negative mode.

The utilization of the different identified formulas and their respective abundances can give further information about the effect of different treatments. We recommend the creation of a model to analyze the different abundances and molecular formulas. Moreover, Van Krevelen diagrams should be created, as they can provide information about the different LDOC and RDOC species.

Finally, there is insufficient understanding of the effects of multi-stressors such as high-pressure, low pH, and high T on the production of RDOC. Studying multi-stressors in the deep sea would allow us to create models to explain the effect of raising T in the oceans and OA on the global pool of marine RDOC. We recommend that further studies address this issue.

11 List of References

Amon, R.M.W., Benner, R., 1996. Bacterial utilization of different size classes of dissolved organic matter. Limnol. Oceanogr. 41, 41–51. https://doi.org/10.4319/lo.1996.41.1.0041

Beman, J.M., Chow, C.-E., King, A.L., Feng, Y., Fuhrman, J. a, Andersson, A., Bates, N.R., Popp, B.N., Hutchins, D.A., 2011. Global declines in oceanic nitrification rates as a consequence of ocean acidification. Proc. Natl. Acad. Sci. 108, 208–213. https://doi.org/10.1073/pnas.1011053108

Blackford, J., Jones, N., Proctor, R., Holt, J., Widdicombe, S., Lowe, D., Rees, A., 2009. An initial assessment of the potential environmental impact of CO_2 escape from marine carbon capture and storage systems. Proc. Inst. Mech. Eng. Part A J. Power Energy 223, 269–280. https://doi.org/10.1243/09576509JPE623

Borrero-Santiago, A.R., Bautista-Chamizo, E., DelValls, T.Á., Riba, I., 2017. A possible CO 2 leakage event: Can the marine microbial community be recovered? Mar. Pollut. Bull. 117, 380–385. https://doi.org/10.1016/j.marpolbul.2017.02.027

Borrero-Santiago, A.R., Carbú, M., DelValls, T.Á., Riba, I., 2016. CO2 leaking from sub-seabed storage: Responses of two marine bacteria strains. Mar. Environ. Res. 121, 2–8. https://doi.org/10.1016/j.marenvres.2016.05.018

Børsheim, K.Y., Myklestad, S.M., Sneli, J.-A., 1999. Monthly profiles of DOC, mono- and polysaccharides at two locations in the Trondheimsfjord (Norway) during two years. Mar. Chem. 63, 255–272. https://doi.org/10.1016/S0304-4203(98)00066-8

Brewer, P.G., 1997. Ocean chemistry of the fossil fuel CO 2 signal: The haline signal of “business as usual.” Geophys. Res. Lett. 24, 1367–1369. https://doi.org/10.1029/97GL01179

Brophy, J.E., Carlson, D.J., 1989. Production of biologically refractory dissolved organic carbon by natural seawater microbial populations. Deep. Res. 36, 497–507.

Carlson, D.J., Mayer, L.M., Brann, M.L., Mague, T.H., 1985. Binding of monomeric organic compounds to macromolecular dissolved organic matter in seawater. Mar. Chem. 16, 141–153.

Crawford Scientific, n.d. Mass Spectrometry [WWW Document]. theory HPLC. URL http://www.ecs.umass.edu/eve/background/methods/chemical/Openlit/Chromacademy LCMS Intro.pdf (accessed 3.9.18).

Dickson, A.G., 1993. The measurement of sea water pH. Mar. Chem. 44, 131–142. https://doi.org/10.1016/0304-4203(93)90198-W

Dickson, A.G., 1981. An exact definition of total alkalinity and a procedure for the estimation of alkalinity and total inorganic carbon from titration data. Deep Sea Res. Part A. Oceanogr. Res. Pap. 28, 609–623. https://doi.org/10.1016/0198-0149(81)90121-7

Dittmar, T., Koch, B., Hertkorn, N., Kattner, G., 2008. A simple and efficient method for the solid-phase extraction of dissolved organic matter (SPE-DOM) from seawater. Limnol. Oceanogr. Methods 6, 230–235.

Doney, S.C., Fabry, V.J., Feely, R.A., Kleypas, J.A., 2009. Ocean Acidification: The Other CO 2 Problem. Ann. Rev. Mar. Sci. 1, 169–192. https://doi.org/10.1146/annurev.marine.010908.163834

Ducklow, H., Steinberg, D., Buesseler, K., 2001. Upper Ocean Carbon Export and the Biological Pump. Oceanography 14, 50–58. https://doi.org/10.5670/oceanog.2001.06

Engel, A., Delille, B., Jacquet, S., Riebesell, U., Rochelle-Newall, E., Terbrüggen, A., Zondervan, I., 2004a. Transparent exopolymer particles and dissolved organic carbon production by Emiliania huxleyi exposed to different CO2 concentrations: A mesocosm experiment. Aquat. Microb. Ecol. 34, 93–104. https://doi.org/10.3354/ame034093

Engel, A., Piontek, J., Grossart, H.P., Riebesell, U., Schulz, K.G., Sperling, M., 2014. Impact of CO2 enrichment on organic matter dynamics during nutrient induced coastal phytoplankton blooms. J. Plankton Res. 36, 641–657. https://doi.org/10.1093/plankt/fbt125

Engel, A., Thoms, S., Riebesell, U., Rochelle-Newall, E., Zondervan, I., 2004b. Polysaccharide aggregation as a potential sink of marine dissolved organic carbon. Nature 428, 27–30. https://doi.org/10.1038/nature02453

Ericksson, L., Byrne, T., Johansson, E., Trygg, J., Vikström, C., 2013. PCA, in: Multi- and Megavariate Data Analysis Basic Principles and Applications. Umetrics Academy, Malmö, p. 521.

Fabry, V.J., Seibel, B.A., Feely, R.A., Orr, J.C., 2008. Impacts of ocean acidification on marine fauna and ecosystem processes. ICES J. Mar. Sci. 65, 414–432. https://doi.org/10.1093/icesjms/fsn048

Feely, R. a, 2004. Impact of Anthropogenic CO2 on the CaCO3 System in the Oceans. Science 305, 362–366. https://doi.org/10.1126/science.1097329

Feely, R., Doney, S., Cooley, S., 2009. Ocean Acidification: Present Conditions and Future Changes in a High-CO2 World. Oceanography 22, 36–47. https://doi.org/10.5670/oceanog.2009.95

Gibbins, J., Chalmers, H., 2008. Carbon capture and storage. Energy Policy 36, 4317–4322. https://doi.org/10.1016/j.enpol.2008.09.058

Global CCS Institute, 2017. Large Scale CCS Projects [WWW Document]. Projects. URL https://www.globalccsinstitute.com/projects/large-scale-ccs-projects (accessed 3.31.17).

Gordon, D.C., 1971. Distribution of particulate organic carbon and nitrogen at an oceanic station in the central Pacific. Deep. Res. 18.

Grossart, H.-P., Allgaier, M., Passow, U., Riebesell, U., 2006. Testing the effect of CO2 concentration on the dynamics of marine heterotrophic bacterioplankton. Limnol. Oceanogr. 51, 1–11. https://doi.org/10.4319/lo.2006.51.1.0001

Grumbach, E.S., Arsenault, J.C., McCabe, D.R., 2012. [Beginners Guide to] UPLC Ultra-Performance Liquid Chromatography.

Hansell, D.A., 2013. Recalcitrant Dissolved Organic Carbon Fractions. Ann. Rev. Mar. Sci. 5, 421–445. https://doi.org/10.1146/annurev-marine-120710-100757

Haszeldine, R.S., 2009. Carbon Capture and Storage: How Green Can Black Be?. Science 325, 1647–1652. https://doi.org/10.1126/science.1172246

Hertkorn, N., Benner, R., Frommberger, M., Schmitt-Kopplin, P., Witt, M., Kaiser, K., Kettrup, A., Hedges, J.I., 2006. Characterization of a major refractory component of marine dissolved organic matter. Geochim. Cosmochim. Acta 70, 2990–3010. https://doi.org/10.1016/j.gca.2006.03.021

Herzog, H., Golomb, D., 2004. Carbon Capture and Storage from Fossil Fuel Use, in: Encyclopedia of Energy. Elsevier, pp. 277–287. https://doi.org/10.1016/B0-12-176480-X/00422-8

Hoffmann, L., Breitbarth, E., Boyd, P., Hunter, K., 2012. Influence of ocean warming and acidification on trace metal biogeochemistry. Mar. Ecol. Prog. Ser. 470, 191–205. https://doi.org/10.3354/meps10082

Iturriaga, R., Zsolnay, A., 1981. Transformation of Some Dissolved Organic Compounds by a Natural Heterotrophic Population. Mar. Biol. 62, 125–129.

James, A.K., Passow, U., Brzezinski, M.A., Parsons, R.J., Trapani, J.N., Carlson, C.A., 2017. Elevated pCO2 enhances bacterioplankton removal of organic carbon. PLoS One 12. https://doi.org/10.1371/journal.pone.0173145

Jiao, N., Herndl, G.J., Hansell, D.A., Benner, R., Kattner, G., Wilhelm, S.W., Kirchman, D.L., Weinbauer, M.G., Luo, T., Chen, F., Azam, F., 2010. Microbial production of recalcitrant dissolved organic matter: long-term carbon storage in the global ocean. Nat. Rev. Microbiol. 8, 593–599. https://doi.org/10.1038/nrmicro2386

Jiao, N., Robinson, C., Azam, F., Thomas, H., Baltar, F., Dang, H., Hardman-Mountford, N.J., Johnson, M., Kirchman, D.L., Koch, B.P., Legendre, L., Li, C., Liu, J., Luo, T., Luo, Y.-W., Mitra, A., Romanou, A., Tang, K., Wang, X., Zhang, C., Zhang, R., 2014. Mechanisms of microbial carbon sequestration in the ocean - future research directions. Biogeosciences 11, 5285–5306. https://doi.org/10.5194/bg-11-5285-2014

Jørgensen, L., Lechtenfeld, O.J., Benner, R., Middelboe, M., Stedmon, C.A., 2014. Production and transformation of dissolved neutral sugars and amino acids by bacteria in seawater. Biogeosciences 11, 5349–5363. https://doi.org/10.5194/bg-11-5349-2014

Karl, T.R., 2003. Modern Global Climate Change. Science 302, 1719–1723. https://doi.org/10.1126/science.1090228

Koch, B.P., Ludwichowski, K.-U., Kattner, G., Dittmar, T., Witt, M., 2008. Advanced characterization of marine dissolved organic matter by combining reversed-phase liquid chromatography and FT-ICR-MS.

Mar. Chem. 111, 233–241. https://doi.org/10.1016/j.marchem.2008.05.008

Kolber, Z., 2007. Energy Cycle in the Ocean: Powering the Microbial World. Oceanography 20, 79–88. https://doi.org/10.5670/oceanog.2007.51

Libes, S., 2009. Production and Destruction of Organic Compounds in the Sea, in: Introduction to Marine Biogeochemistry. Academic Press, p. 928.

MacGilchrist, G.A., Shi, T., Tyrrell, T., Richier, S., Moore, C.M., Dumousseaud, C., Achterberg, E.P., 2014. Effect of enhanced pCO2 levels on the production of DOC and TEP in short-term bioassay experiments. Biogeosciences Discuss. 11, 3701–3730. https://doi.org/10.5194/bgd-11-3701-2014

Martín-Torre, M.C., Payán, M.C., Galán, B., Coz, A., Viguri, J.R., 2013. The use of leaching tests to assess metal release from contaminated marine sediment under CO2 leakages from CCS. Energy Procedia 51, 40–47. https://doi.org/10.1016/j.egypro.2014.07.005

Metz, B., Davidson, O., de Coninc, H., Loos, M., Meyer, L. (Eds.), 2005. IPCC Special Report on Carbon Dioxide Capture and Storage. Cambridge University Press, Cambridge.

Molari, M., Guilini, K., Lott, C., Weber, M., Beer, D. de, Meyer, S., Ramette, A., Wegener, G., Wenzhöfer, F., Martin, D., Cibic, T., Vittor, C. De, Vanreusel, A., Boetius, and A., 2018. CO2 leakage alters biogeochemical and ecological functions of submarine sands. Sci. Adv. 4. https://doi.org/10.1126/sciadv.aao2040

Mopper, K., Zhou, X., Kieber, R.J., Kieber, D.J., Sikorski, R.J., Jones, R.D., 1991. Photochemical degradation of dissolved organic carbon and its impact on the oceanic carbon cycle. Nature 353, 60–62. https://doi.org/10.1038/353060a0

Mucci, A., 1983. The solubility of calcite and aragonite in seawater at various salinities, temperatures, and one atmosphere total pressure. Am. J. Sci. 283, 780–799. https://doi.org/10.2475/ajs.283.7.780

Nalewajko, C., 1977. Extracellular release in freshwater algae and bacteria: extracellular products of algae as a source of carbon for heterothrophs, in: Cairns, J. (Ed.), Aquatic Microbial Communities. Garland Pub., New York, pp. 589–626.

National Oceanic and Atmospheric Administration, 2017. Recent Monthly Average Mauna Loa CO2 [WWW Document]. Trends Atmos. Carbon Dioxide. URL https://www.esrl.noaa.gov/gmd/ccgg/trends/ (accessed 3.27.17).

Nonlinear Dynamics, 2015. Progenesis QI v2.3.

OCB, 2009. Responses to EPA Notice of Data Availability From Ocean Carbon and Biogeochemistry Program. North.

Ogawa, H., 2001. Production of Refractory Dissolved Organic Matter by Bacteria. Science 292, 917–920. https://doi.org/10.1126/science.1057627

Ogawa, H., Tanoue, E., 2003. Dissolved Organic Matter in Oceanic Waters. J. Oceanogr. 59, 129–147. https://doi.org/10.1023/A:1025528919771

Orr, J.C., Fabry, V.J., Aumont, O., Bopp, L., Doney, S.C., Feely, R.A., Gnanadesikan, A., Gruber, N., Ishida, A., Joos, F., Key, R.M., Lindsay, K., Maier-Reimer, E., Matear, R., Monfray, P., Mouchet, A., Najjar, R.G., Plattner, G.-K., Rodgers, K.B., Sabine, C.L., Sarmiento, J.L., Schlitzer, R., Slater, R.D., Totterdell, I.J., Weirig, M.-F., Yamanaka, Y., Yool, A., 2005. Anthropogenic ocean acidification over the twenty-first century and its impact on calcifying organisms. Nature 437, 681–686. https://doi.org/10.1038/nature04095

Peterson, C.K., 2016. Influence of siderophore-iron complexation on the growth of the diatom Skeletonema costatum: a mass spectroscopy approach. Norwegian University of Science and Technology.

Pierrot, D., Lewis, E., Wallace, D.W.R., 2006. MS Excel Program Developed for CO2 System Calculations. https://doi.org/10.3334/CDIAC/otg.CO2SYS_XLS_CDIAC105a

Piontek, J., Borchard, C., Sperling, M., Schulz, K.G., Riebesell, U., Engel, A., 2013. Response of bacterioplankton activity in an Arctic fjord system to elevated pCO2: results from a mesocosm perturbation study. Biogeosciences 10, 297–314. https://doi.org/10.5194/bg-10-297-2013

Piontek, J., Lunau, M., Händel, N., Borchard, C., Wurst, M., Engel, A., 2010. Acidification increases microbial polysaccharide degradation in the ocean. Biogeosciences 7, 1615–1624. https://doi.org/10.5194/bg-7-1615-2010

Prichard, E., Lawn, R., 2003. Measurement of pH. Royal Society of Chemistry.

Reimer, A., Arp, G., 2011. Alkalinity, in: Reitner, J., Thiel, V. (Eds.), Encyclopedia of Geobiology, Encyclopedia of Earth Sciences Series. Springer Netherlands, Dordrecht. https://doi.org/10.1007/978-1-4020-9212-1

Riebesell, U., Gattuso, J.P.P., Thingstad, T.F.F., Middelburg, J.J.J., 2013. Arctic ocean acidification : pelagic ecosystem and biogeochemical Dynamics responses during a mesocosm study. Biogeosciences 10, 5619–5626. https://doi.org/10.1594/PANGAEA.769833

Ries, J.B., Cohen, A.L., McCorkle, D.C., 2009. Marine calcifiers exhibit mixed responses to CO2-induced ocean acidification. Geology 37, 1131–1134. https://doi.org/10.1130/G30210A.1

Roggatz, C.C., Lorch, M., Hardege, J.D., Benoit, D.M., 2016. Ocean acidification affects marine chemical communication by changing structure and function of peptide signalling molecules. Glob. Chang. Biol. 22, 3914–3926. https://doi.org/10.1111/gcb.13354

Sabine, C.L., 2004. The Oceanic Sink for Anthropogenic CO2. Science 305, 367–371. https://doi.org/10.1126/science.1097403

Saunders, G.W., 1977. Carbon flow in the aquatic system, in: Cairns, J. (Ed.), Aquatic Microbial Communities. Garland Pub., New York, pp. 417–439.

Sharp, J.H., 1973. Size classes of organic. Limnol. Oceanogr. 18, 441–447.

Søndergaard, M., Middelboe, M., 1995. A cross-system analysis of labile dissolved organic carbon *. Mar. Ecol. Prog. Ser. 118, 283–294.

Starmer, J., 2015. StatQuest: Principal Component Analysis (PCA) clearly explained [WWW Document]. URL https://www.youtube.com/watch?v=_UVHneBUBW0 (accessed 4.22.18).

SUEZ, n.d. About Total Organic Carbon (TOC) [WWW Document]. TOC Anal. Buyer´s Guid. URL https://www.geinstruments.com/library/about-total-organic-carbon-toc (accessed 3.9.18).

Teledyne Tekmar, n.d. Apollo 9000 TN [WWW Document]. Discontin. Prod. URL http://www.teledynetekmar.com/prods/discontinuedProducts/Pages/Apollo-9000.aspx (accessed 3.9.18).

University of Gdansk, 2013. Impact of potential leakage from the sub-seabed CO2 storage site on marine environment at relevant hydrostatic pressure [WWW Document]. About CO2 Mar. URL http://co2marine.ug.edu.pl/?page_id=28 (accessed 3.31.17).

Verma, N., 2012. Elemental Analyzer [WWW Document]. Elem. Anal. URL https://www.iitk.ac.in/dordold/index.php?option=com_content&view=category&layout=blog&id=222&Itemid=241 (accessed 3.14.18).

Williams, P., Carlucci, A., Henrichs, S., Van Vleet, E., Horrigan, S., Reid, F.M., Robertson, K., 1986. Chemical and microbiological studies of sea-surface films in the Southern Gulf of California and off the West Coast of Baja California. Mar. Chem. 19, 17–98. https://doi.org/10.1016/0304-4203(86)90033-2

Williams, R.G., Follows, M.J., 2011. Ocean Dynamics and the Carbon Cycle: Principles and Mechanisms. Cambridge University Press.

Wolf- Gladrow, D.A., Zeebe, R.E., Klaas, C., Körtzinger, A., Dickson, A.G., 2007. Total alkalinity: The explicit conservative expression and its application to biogeochemical processes. Mar. Chem. 106, 287–300. https://doi.org/10.1016/j.marchem.2007.01.006

Yamada, N., Tsurushima, N., Suzumura, M., 2013. Effects of CO2-Induced Seawater Acidification on Microbial Processes Involving Dissolved Organic Matter. Energy Procedia 37, 5962–5969. https://doi.org/10.1016/j.egypro.2013.06.523

Zark, M., Riebesell, U., Dittmar, T., 2015. Effects of ocean acidification on marine dissolved organic matter are not detectable over the succession of phytoplankton blooms. Sci. Adv. 1, e1500531–e1500531. https://doi.org/10.1126/sciadv.1500531

Appendix: Tables and Figures

DOC control experiment

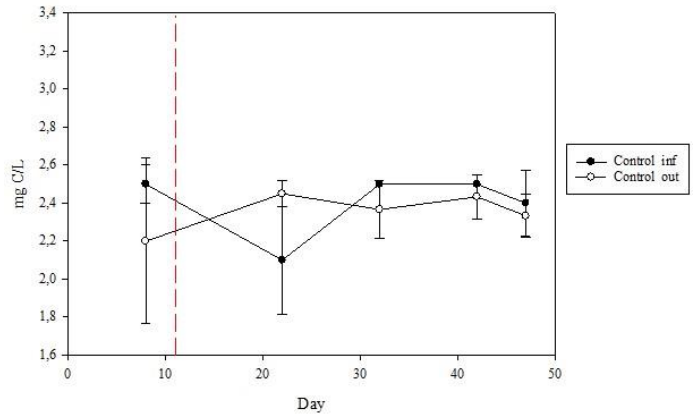

Fig. 11.1 Comparison between the inflow and outflow DOC of the control experiment

DOC pH 7 experiment

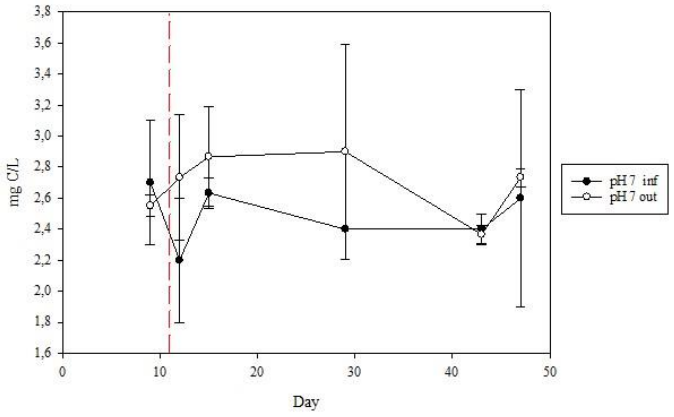

Fig. 11.2 Comparison between the inflow and outflow DOC of the pH 7 experiment

POC control experiment

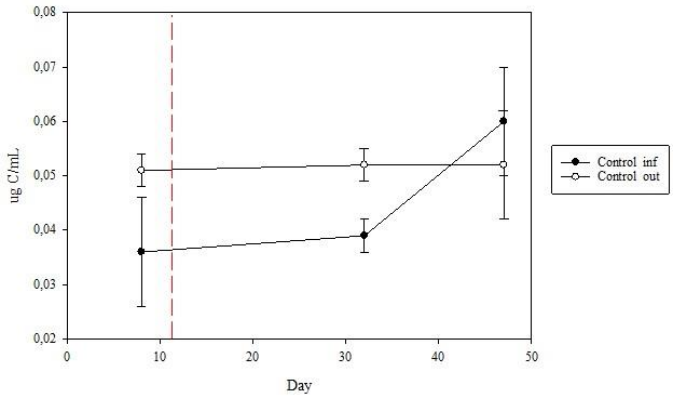

Fig. 11.3 Comparison between the inflow and outflow POC of the control experiment

POC pH 7 experiment

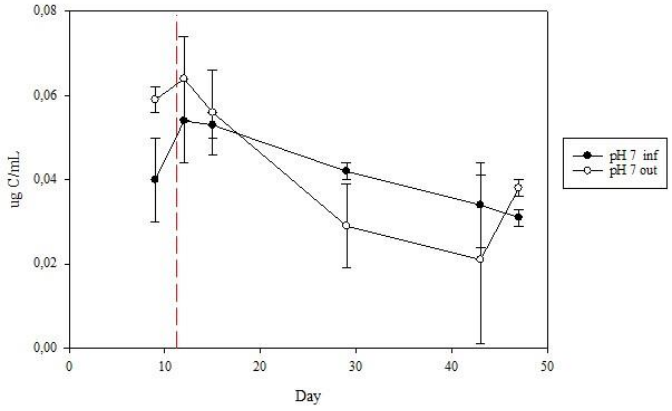

Fig. 11.4 Comparison between the inflow and outflow POC of the pH 7 experiment

DOC BD control experiment

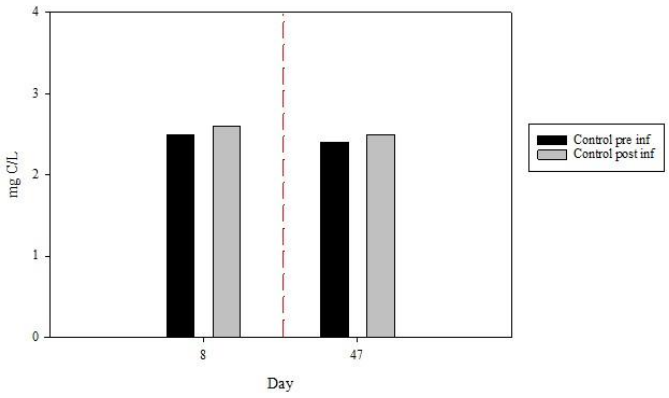

Fig. 11.5 Comparison between the pre and post BD inflow DOC during the control experiment

DOC BD pH 7 experiment

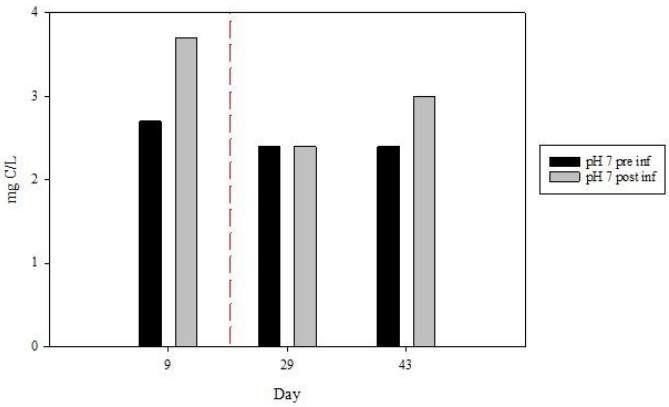

Fig. 11.6 Comparison between pre and post BD inflow DOC during the pH 7 experiment

POC BD control experiment

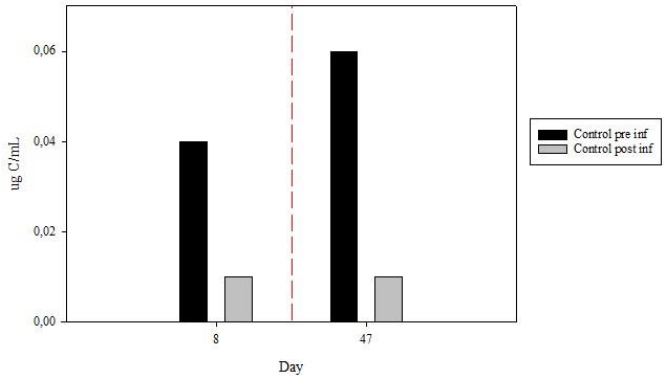

Fig. 11.7 Comparison between the pre and post BD inflow POC during the control experiment

POC BD pH 7 experiment

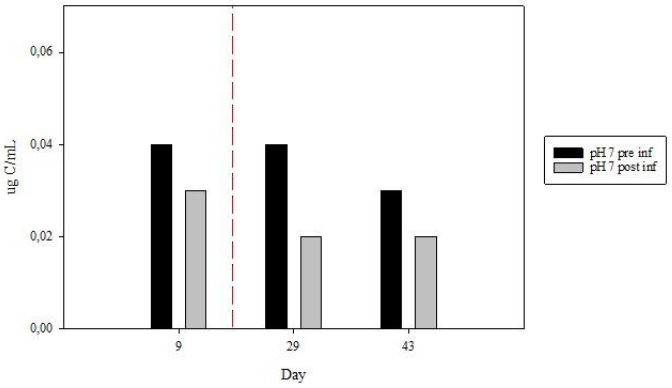

Fig. 11.8 Comparison between pre and post BD inflow POC during the pH 7 experiment

DOC/C of the BD samples

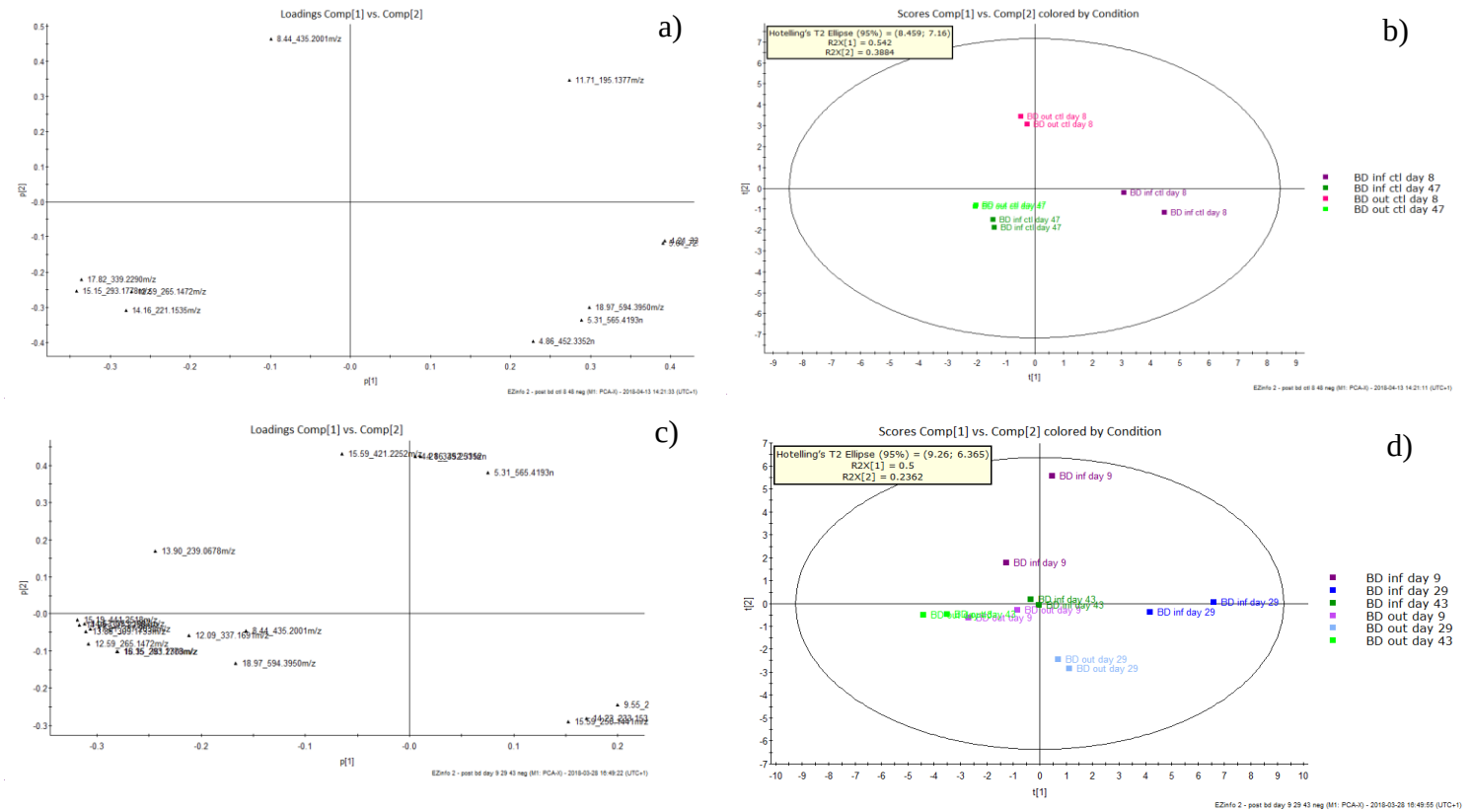

Fig. 11.9 Inflow and outflows after BD negative mode
Control a) loadings and b) scores and pH 7 experiment c) loadings and d) scores

DOC/C: identifications

pH 7 experiment

Table 11.1 pH7 experiment identified compounds, positive mode
MW: molecular weight, red line symbolizes the start of the addition of CO_2.

MW	Formula	Inf day 9	Out day 9	Inf day 12	Out day 12	Inf day 15	Out day 15	Inf day 29	Out day 29	Inf day 47	Out day 47
114.0911	C6H11NO			x		x					
114.0912	C5H7N			x		x		x		x	
133.0138	C5H2N4O2						x				
207.0324	C9H7N2O2P						x				
209.1638	C6H21N6P			x		x					
219.173	C9H23N4P								x		
227.1753	C12H22N2O2			x		x		x			
233.2008	C13H21N										x
242.174	C9H19N3O2			x							
251.0465	C12H11O4P				x						
256.1517	C17H23NS			x		x					
271.1868	C12H26N4				x						
274.7121	C30H53N5O4			x		x					
277.1777	C12H29N2P				x						
284.2941	C16H34O								x		
291.1925	C8H23N10P				x						
305.1523	C5H20N8O7				x						
312.2273	C9H26N7OP				x		x				
313.2734	C18H32O2				x						
322.2483	C19H35N			x		x					
330.2382	C13H26N6		x		x		x		x		
331.2541	C36H64N6O5			x		x		x			
340.2601	C16H38NO4P			x		x					
341.2633	C6H14N6			x		x					
346.2673	C11H28N8O2			x		x					
354.2749	C14H35N4P			x		x					
362.2418	C12H34N7O2P			x							
372.285	C16H32N6			x		x					
372.2857	C17H34N2O4			x		x					
396.8021	C42H77N7O7			x		x					

MW	Formula	Inf day 9	Out day 9	Inf day 12	Out day 12	Inf day 15	Out day 15	Inf day 29	Out day 29	Inf day 47	Out day 47
401.2627	C21H40O4			x		x					
443.3229	C20H39N3O5				x		x				
453.3447	C22H49N2O5P			x		x					
459.3516	C21H48N4O5			x		x					
485.3703	C20H48N5O2P			x		x					
491.2993	C21H39N4O5P			x		x					
566.4291	C28H60N3O6P			x		x					
610.1851	C44H26N3P		x								
701.4942	C34H71N4O7P			x		x					

Table 11.2 pH7 experiment identified compounds, negative mode
MW: molecular weight, red line symbolizes the start of the addition of CO_2

MW	Formula	Inf day 9	Out day 9	Inf day 12	Out day 12	Inf day 15	Out day 15	Inf day 29	Out day 29	Inf day 47	Out day 47
149.0088	C4H6O6							x			
165.0396	C9H14P2							x			
183.0114	C6H12OP2	x									
183.0115	C10H5N2P	x				x					
195.1377	C7H20N4		x								
221.1538	C9H22N4		x								
223.027	C14H6N2							x			
223.0272	C11H16P2S							x			
236.1047	C12H13N7		x								
239.0207	C11H4N4O3			x							
255.2315	C12H28N6		x								
265.1472	C11H24N4S			x					x		
283.0102	C15H8N2S			x							
283.1537	C12H18N10		x				x				
288.9753	C9H7O9P			x							
293.1751	C12H26N4O2		x								
297.1524	C11H26N4OS	x				x					
299.2574	C14H32N6O		x								
311.1683	C16H26OS	x				x					
325.1843	C17H28OS	x				x					
325.2491	C13H34N6O	x				x					
337.1691	C14H30N4P2		x		x		x		x		x
339.1988	C17H36OP2		x								
339.1992	C14H32N4OS	x				x					
355.1578	C21H24N2O		x								
361.1637	C8H11N3O2		x								
363.1846	C16H32N4P2		x				x		x		x
374.131	C12H19N5O6		x					x			
384.2496	C18H33N3O3				x		x		x		x
421.2252	C15H34N6OP2					x					
435.2001	C8H10N8		x		x		x				
497.3343	C23H48O8			x		x		x			
594.395	C27H59N7OP2							x			
610.4183	C30H55N5O5	x		x		x		x		x	
723.5026	C34H71N8O5P	x		x		x		x		x	

BD experiment

Table 11.3 Pre and post BD identified compounds from the pH 7 experiment day 9 and 29, positive mode
MW: molecular weight, red line symbolizes the start of the addition of CO_2

MW	Formula	Pre inf day 9 10/11	Post inf day 9 15/11	Pre out day 9 10/11	Post out day 9 15/11	Pre inf day 29 30/11	Post inf day 29 05/12	Pre out day 29 30/11	Post out day 29 05/12
93.0334	C6H4O					x			
114.0911	C6H11NO			x			x	x	
114.0912	C5H7N			x		x		x	
121.0287	C7H4O2				x	x			
149.0236	C8H4O3				x	x			
204.1382	C11H14O					x			
207.0324	C9H7N2O2P			x					
209.1638	C6H21N6P					x			
219.1734	C9H23N4P				x	x			
227.1753	C12H22N2O2							x	
233.2008	C13H21N				x	x			
240.2321	C13H26O						x		
256.1517	C17H23NS			x			x		
266.9994	C18H3OP								x
268.9796	C16H2N2O2S			x					
274.7121	C30H53N5O4					x			
281.0515	C10H16O5S2			x					
298.3466	C20H43N		x		x				
310.3098	C20H39NO						x		
312.2273	C9H26N7OP		x				x		
322.2483	C19H35N					x			
326.3775	C22H47N		x						
330.2382	C13H26N6		x				x		
331.2541	C36H64N6O5			x		x			
331.3105	C20H35N		x		x	x			
340.2601	C18H33N3O3					x			
341.0181	C18H10N2S2			x					
346.2673	C11H28N8O2	x				x			
354.2749	C14H35N4P	x				x			
372.285	C16H32N6	x				x			
393.2066	C20H28NOP						x		
395.2093	C9H26N6O9		x				x		

MW	Formula	Pre inf day 9 10/11	Post inf day 9 15/11	Pre out day 9 10/11	Post out day 9 15/11	Pre inf day 29 30/11	Post inf day 29 05/12	Pre out day 29 30/11	Post out day 29 05/12
396.8021	C42H77N7O7					x			
401.2627	C21H40O4	x				x		x	
429.0888	C28H18N2S2			x					
443.3229	C20H39N3O5		x				x		
453.3447	C22H49N2O5P					x			
459.3516	C21H48N4O5	x				x			
485.3703	C20H48N5O2P					x			
491.2993	C21H39N4O5P					x			
566.4291	C28H60N3O6P					x			
701.4942	C34H71N4O7P					x			

Table 11.4 Pre and post BD identified compounds from the pH 7 experiment day 9 and 29, negative mode
MW: molecular weight, red line symbolizes the start of the addition of CO_2

MW	Formula	Pre inf day 9 10/11	Post inf day 9 15/11	Pre out day 9 10/11	Post out day 9 15/11	Pre inf day 29 30/11	Post inf day 29 05/12	Pre out day 29 30/11	Post out day 29 05/12
149.0088	C4H6O6			x					
165.0396	C9H14P2			x					
183.0112	C6H12OP2				x		x		
195.1377	C7H20N4					x			
221.1535	C9H22N4			x		x			
223.0272	C11H16P2S			x					
223.0277	C14H6N2			x					
236.1047	C12H13N7			x					
239.0207	C11H4N4O3		x			x			
239.0678	C5H9N10P		x		x				
250.1441	C9H21N5O					x			
255.2315	C12H28N6					x			
283.0102	C15H8N2S					x			
283.1537	C12H18N10		x		x				
288.9753	C9H7O9P		x			x		x	
293.1751	C12H26N4O2			x					
297.1524	C11H26N4OS				x		x		
299.2574	C14H32N6O			x		x			
311.1683	C16H26OS				x				
325.1843	C17H28OS				x				
325.2491	C13H34N6O				x		x		
337.1691	C14H30N4P2					x		x	
339.1988	C17H36OP2		x						
339.1992	C14H32N4OS				x		x		
339.229	C18H32N2O4		x						
355.1578	C21H24N2O			x		x			
361.1637	C8H11N3O2		x						
363.1846	C16H32N4P2					x		x	
374.131	C12H19N5O6			x		x			
384.2496	C18H33N3O3			x		x		x	
421.2252	C15H34N6OP2			x		x		x	
435.2001	C8H10N8		x			x			
497.3343	C23H48O8			x		x		x	

MW	Formula	Pre inf day 9 10/11	Post inf day 9 15/11	Pre out day 9 10/11	Post out day 9 15/11	Pre inf day 29 30/11	Post inf day 29 05/12	Pre out day 29 30/11	Post out day 29 05/12
594.395	C27H59N7OP2			x		x		x	
610.4183	C30H55N5O5			x		x		x	
723.5026	C34H71N8O5P			x		x		x	

Table 11.5 Comparison between the inflow and outflow post BD samples from day 9, 29 and 43 positive mode
MW: molecular weight, red line symbolizes the start of the addition of CO_2

MW	Formula	Post inf day 9 15/11	Post out day 9 15/11	Post inf day 29 05/12	Post out day 29 05/12	Post inf day 43 19/12	Post out day 43 19/12
93.0334	C6H4O		x				
114.0913	C5H7N	x			x		
121.0287	C7H4O2		x				
133.0138	C5H2N4O2						x
149.0236	C8H4O3		x				
207.0324	C9H7N2O2P						x
209.1638	C6H21N6P		x				
219.1734	C9H23N4P				x		
219.1737	C15H22O				x		
227.1753	C12H22N2O2	x	x				
233.2008	C13H21N			x	x		
235.1679	C9H19N3O2				x		
242.174	C19N3O2	x	x				
245.08	C11H7N3		x				
274.7121	C30H53N5O4				x		
298.3466	C20H43N	x	x				
305.1523	C5H20N8O7		x				
312.2273	C9H26N7OP						x
313.2734	C18H32O2						x
322.2483	C19H35N	x					
326.3775	C22H47N		x				
330.2382	C13H26N6		x				
331.2541	C36H64N6O5				x		
331.3105	C20H35N	x			x		
340.2601	C18H33N3O3	x					x
341.0181	C23H10N2P2						x
341.2633	C6H14N6		x				
346.2673	C11H28N8O2		x				
349.1792	C23H24O3		x				
355.135	C6H11NO5				x		
372.285	C16H32N6		x				
381.2883	C23H38N2O		x				
393.2066	C20H28NOP		x				
396.8021	C42H77N7O7				x		
437.2327	C28H28N4O		x				
443.3229	C20H39N3O5		x				
453.3447	C22H49N2O5P				x		
459.3516	C21H48N4O5						x
485.3703	C20H48N5O2P						x

MW	Formula	Post inf day 9 15/11	Post out day 9 15/11	Post inf day 29 05/12	Post out day 29 05/12	Post inf day 43 19/12	Post out day 43 19/12
491.2993	C21H39N4O5P	x					
566.4291	C28H60N3O6P				x		
575.1051	C44H14O2						x
701.4942	C34H71N4O7P				x		

Table 11.6 Comparison between the inflow and outflow post BD samples from day 9, 29 and 43 negative mode
MW: molecular weight, red line symbolizes the start of the addition of CO_2

MW	Formula	Post inf day 9 15/11	Post out day 9 15/11	Post inf day 29 05/12	Post out day 29 05/12	Post inf day 43 19/12	Post out day 43 19/12
183.0112	C6H12OP2		x				
183.0115	C10H5N2P		x				
221.1535	C9H22N4						x
233.1535	C9H23N4OP			x	x		
236.1047	C12H13N7						x
239.0207	C11H4N4O3	x					
239.0678	C5H9N10P	x	x				
250.1441	C9H21N5O			x	x		
265.1472	C11H24N4S					x	
283.1537	C12H18N10			x	x		
288.9753	C9H7O9P	x					
293.1751	C12H26N4O2						x
311.1683	C16H26OS		x				
325.1843	C17H28OS		x				
337.2038	C12H32N6OP2						x
339.1992	C14H32N4OS		x				
384.2496	C18H33N3O3	x	x				
421.2252	C15H34N6OP2						x
435.2001	C8H10N8	x	x				
441.2518	C15H38N6O2P2						x
497.3343	C23H48O8	x					
594.395	C27H59N7OP2						x
610.4183	C30H55N5O5				x		
723.5026	C34H71N8O5P				x		